HHS Public Access

Author manuscript

Eur Radiol. Author manuscript; available in PMC 2024 August 01.

Published in final edited form as:

Eur Radiol. 2023 August ; 33(8): 5309–5320. doi:10.1007/s00330-023-09596-y.

Clinical Applications of Photon Counting Detector CT

Cynthia H. McCollough, Ph.D.[1], **Kishore Rajendran, Ph.D.**[1], **Francis I. Baffour, M.D.**[1], **Felix E. Diehn, M.D.**[1], **Andrea Ferrero, Ph.D.**[1], **Katrina N. Glazebrook, M.B., Ch.B.**[1], **Kelly K. Horst, M.D.**[1], **Tucker F. Johnson, M.D.**[1], **Shuai Leng, Ph.D.**[1], **Achille Mileto, M.D.**[1], **Prabhakar Shantha Rajiah, Ph.D.**[1], **Bernhard Schmidt, Ph.D.**[2], **Lifeng Yu, Ph.D.**[1], **Thomas G. Flohr, Ph.D.**[2], **Joel G. Fletcher, M.D.**[1]

[1]Department of Radiology, Mayo Clinic, Rochester, MN, USA

[2]Siemens Healthineers, Forchheim, Germany

Abstract

The x-ray detector is a fundamental component of a CT system that determines image quality and dose efficiency. Until the approval of the first clinical photon-counting-detector (PCD) system in 2021, all clinical CT scanners used scintillating detectors, which do not capture information about individual photons in the two-step detection process. In contrast, PCDs use a one step process whereby x-ray energy is converted directly into electrical signal. This preserves information about individual photons such that the numbers of x-rays in different energy ranges can be counted. Primary advantages of PCDs include the absence of electronic noise, improved radiation dose efficiency, increased iodine signal and the ability to use lower doses of iodinated contrast material, and better spatial resolution. PCDs with more than one energy threshold can sort the detected photons into two or more energy bins, making energy resolved information available for all acquisitions. This allows for material classification or quantitation tasks to be performed in conjunction with high spatial resolution, and in the case of dual-source CT, high pitch or high temporal resolution acquisitions. Some of the most promising applications of PCD-CT involve imaging of anatomy where exquisite spatial resolution adds clinical value. These include imaging of the inner ear, bones, small blood vessels, heart, and lung. This review describes the clinical benefits observed to date and future directions for this technical advance in CT imaging.

MeSH key terms:

Tomography; X-Ray Computed; Radiation Dosage; Humans; Photons; Iodine

Introduction

The beneficial characteristics of photon-counting detectors (PCDs) relative to energy-integrating detectors (EIDs) include the absence of electronic noise, increased iodine signal-to-noise-ratio (SNR) due to equivalent weighting of low- and high-energy photons, the ability to decrease detector pixel size without loss of radiation dose efficiency, the ability to

Corresponding Author: Cynthia H. McCollough, PhD, 200 First Street SW, Rochester, MN 55905, Phone: (507) 538-0633, Fax: (507) 266-3661, mccollough.cynthia@mayo.edu.

bin photons according to their respective energies to facilitate multi-energy applications, and the ability to differentiate high atomic number contrast agents having sufficiently different k-edges (e.g., iodine versus gadolinium or bismuth). These and other technical characteristics are reviewed in part one of this review [1], which explains the physical basis for the improvements in image quality and dose efficiency. In this work, we review how the technical characteristics of PCDs have been translated into the clinic to improve diagnostic capabilities, improve radiologist confidence, and benefit patients.

The first human images from PCD-CT were acquired in 2007 using a proof-of-concept PCD-CT system manufactured by General Electric [2]. In 2015, human studies commenced on an investigational dual-source CT system manufactured by Siemens Healthcare [3–5]. The focus of these early clinical studies was to demonstrate the hypothesized benefits of PCD-CT in humans. An investigational human system was developed by Philips Healthcare [6], as well as a second research system from Siemens [7; 8]. Collectively, the studies performed using these systems provided convincing evidence that the anticipated benefits to CT imaging from the use of PCDs could be realized in patients.

In 2021, the first PCD-CT system approved for clinical use was released (NAEOTOM Alpha, Siemens Healthcare) [9]. In 2022, Neurologica announced U.S. FDA 510k clearance of a PCD system for head scanning, the OmniTom Elite. Other CT manufacturers have presented data from prototype PCD systems, which are still in the development or evaluation phase.

Improved Image Quality and Associated Clinical Benefits

Noise

Electronic noise, which can become significant when the signal to the detector is very low, is absent in PCD-CT [1; 10]. This is particularly beneficial for low-dose and quantitative applications. For example, using low-dose PCD-CT, Symons et al. found increased CT number accuracy and stability [11] and lower image noise compared with EID-CT performed using the same radiation dose, while achieving better diagnostic quality and lung nodule contrast-to-noise ratio (CNR) [12].

Radiation dose

Because PCDs do not require septa within the detector layer, as do EIDs, they are inherently more dose efficient. Leng et al. [13] demonstrated that PCD-CT can achieve the same spatial resolution (slice thickness and in-plane resolution) and image noise as EID-CT using a lower radiation dose, as have other investigators [14–18].

Iodine enhancement

The increased enhancement of iodine that occurs with PCD-CT allows for lower volumes of iodinated contrast. This is due to photon counting’s equal weighting of all photon energies (as compared to EID-CT, where the iodine-information-carrying lower-energy photons produce lower detector signal than the higher-energy photons that carry little iodine information). Sawall et al. estimated that a reduction in iodinated contrast volume of up to

13–37% is feasible, with the greatest reduction seen in larger patient sizes [19]. Further, low-energy virtual monoenergetic images (VMIs), which are available for any PCD-CT acquisition using 2 or more energy thresholds, increase iodine signal, enable use of lower doses of iodinated contrast media, and can help salvage suboptimal enhanced vascular studies due to the higher iodine signal [20]. In the absence of reduced doses of iodinated contrast, subtle CT number differences between pathologies are better demonstrated with PCDs owing to the increased iodine signal associated with the equal weighting of low energy photons.

Spatial resolution

The increased spatial resolution of PCD-CT is attractive for most organ systems and radiology subspecialities, including

- CT angiography (CTA) [21; 22];
- temporal bone imaging [23; 24] (Fig. 1);
- visualization of small pulmonary vascular and interstitial structures (Fig. 2) [25; 26];
- visualization of coronary arteries [27; 28], calcifications [29], and stents [30]; and
- visualization of musculoskeletal anatomy and pathology [16; 31–33].

Multi-energy imaging

In EID-CT, quantitative imaging is available using dual-energy acquisitions in specific modes or configurations [34; 35]. PCDs with more than one energy threshold can sort the detected photons into two or more energy bins, making energy-resolved information available for all acquisitions. This multi-energy information can be used to produce images that help distinguish material types and quantify their mass densities. For instance, multi-energy PCD-CT data can be decomposed into iodine maps to quantitate iodine concentrations [36], e.g., within hyper-enhancing lesions [37]. In addition, the x-ray energy discriminating capabilities of PCDs allow for K-edge imaging of high-atomic-number contrast agents (e.g., bismuth, tungsten, gadolinium) by setting the acquisition energy thresholds around the k-edge energies [38].

While many multi-energy applications are similar to dual-energy CT, dual-source PCD-CT permits multi-energy imaging at high pitch (e.g., 3.2) or high temporal resolution (e.g., 66 ms), which are not possible with dual-source EID-CT. However, as high spatial resolution image reconstruction kernels increase image noise, multi-energy reconstructions with these kernels may be of limited value due to the increased noise associated with multi-energy processing.

Metal artifacts and beam hardening

Higher-energy x-rays better penetrate metal and are subject to less beam hardening and scatter. Thus, PCD-CT's ability to produce images derived from only the higher energies of the x-ray beam (e.g., high-energy threshold images) allows for decreased metal artifacts

and beam hardening, which is advantageous for imaging around dense structures or devices such as stents, coils, dental amalgam, or orthopaedic hardware [18]. When combined with dedicated x-ray beam shaping techniques such as pre-patient filtration (e.g., 0.4 mm tin), the low-energy photons that are most affected by beam hardening are filtered out of the x-ray spectrum while also increasing the dose efficiency of the acquisition [39].

VMIs and material decomposition are alternative multi-energy visualization techniques that may result in effective correction of metal artifacts. Importantly, these multi-energy methods are fully compatible with sinogram-based metal artifact reduction algorithms [40].

Organ-system-specific benefits

The body of literature demonstrating clinical benefits from PCD-CT for specific imaging tasks continues to grow. The following sections highlight studies specific to various organ systems.

Neurologic imaging

Using theoretical simulations and benchtop experiments with an anthropomorphic cerebral angiographic phantom, Harvey et al. demonstrated that compared with EID-CT, PCD-CT provided superior vessel conspicuity and reduced artifactual stenoses [21]. In human studies, Symons et al. performed vascular imaging of the head and neck [22] on sixteen asymptomatic subjects using both EID-CT and PCD-CT. PCD-CT image quality scores were significantly higher compared to EID-CT and PCD-CT demonstrated lower image noise and less image artifacts.

In high-spatial-resolution, non-contrast imaging of the temporal bones, both cadaveric and human subject studies demonstrated superior visualization of critical anatomic structures [23; 24]. For example, stapes prostheses that were barely visible at EID-CT were well visualized at PCD-CT. Further, the addition of a tin filter in the beam resulted in dose reductions of up to 85% for imaging of the temporal bone and sinuses [17; 18]. While the use of a tin filter is not unique to PCD-CT, it is synergistic with PCD's equal weighting of all photon energies; the lower energy photons that are detected are not "down-weighted" as they are in EID-CT. Campeau et al. have recently demonstrated that PCD-CTA can display many small periorbital vessels, which are difficult to appreciate at conventional CT [41].

Thoracic imaging

In a study by Inoue et al., who assessed 30 patients with known or suspected interstitial lung disease (ILD) with both an EID-CT system and a PCD-CT, PCD-CT significantly increased reader confidence for the presence or absence of imaging findings of reticulation, ground-glass opacity and mosaic attention, all of which contributed to more accurate categorization of ILD [42]. The use of smaller detector pixels on PCD-CT has been shown to improve the conspicuity of ILD and small bronchi. Alternatively, Jungblut et al. have shown that sensitivity for ILD detection can be maintained despite substantial radiation dose reduction [15]. Similarly, PCD-CT permits radiation dose reduction for contrast-enhanced chest CT while improving contrast-to noise ratio for vessels, pulmonary parenchyma, and pulmonary metastases [14].

With the simultaneous acquisition of high spatial resolution and multi-energy data, PCD-CT allows quantitative display of pulmonary blood pool within the lungs as a complement to the high-resolution anatomical information in patients with suspected acute or chronic pulmonary embolism [43]. As the size of the detector readout pixel is decreased, the rate of data coming from the detector increases, requiring higher data transfer speeds. In some cases, if the maximum bandwidth is exceeded, trade-offs may be required in other aspects of the acquisition, such as longitudinal beam coverage.

Cardiovascular imaging

PCD-CT is particularly advantageous in cardiovascular imaging for the visualization of small vessels [27; 28]. The improved spatial resolution also reduces calcium blooming artifact [29], improving luminal assessment adjacent to dense calcifications and within stents (Fig. 3a–b) [28; 30]. It is anticipated that this will help in the characterization of atherosclerotic plaques [28; 44].

Dual-source CT with EIDs permits either dual-energy or 66 ms temporal resolution imaging; they cannot, however, be performed simultaneously. In dual-source PCD-CT, 66 msec, multi-energy scanning is possible, which allows for material decomposition to remove calcium signal [45] (Fig. 3c–d) to help improve luminal assessment in the presence of dense calcium. High-energy VMIs, e.g., 100 keV, can also be used to decrease artifacts such as from calcium blooming, beam hardening, or metal [46]. Simultaneous use of multi-energy information is also useful in cardiac CT to generate iodine maps reflecting parenchymal perfusion, e.g., delayed iodine CT for myocardial scar, or to calculate extracellular volume [27]. Finally, in work by Symons et al, multi-contrast imaging of the heart has been investigated [47] in a canine model.

Abdominopelvic imaging

In Decker et al., 20 patients with clinically indicated low-dose CT were scanned on a PCD-CT and their images compared with those from a BMI-matched EID-CT-cohort [48]. Image noise was found to be significantly lower and iodine SNR was significantly higher at PCD-CT. Subjective image quality was substantially higher and conspicuity better for the renal pelvis, ureters, and mesenteric vessels on the PCD-CT. There was no significant difference in the conspicuity of the adrenal glands [48]. Higashigaito et al. showed that PCD-CT low energy (50 keV) VMIs resulted in higher iodine CNRs at similar subjective image quality as compared to EID-CT using identical radiation doses [49]. Similar results have been attained within other abdominal tasks, such as detection of peritoneal carcinomatosis where visualization of small peritoneal or serosal deposits is enhanced using PCD-CT (Fig. 4a–c). Through the substantial increase in iodine CNR, PCD-CT has notable relevance in efforts to achieve similar diagnostic-quality images with reduced radiation [48] or iodine doses.

PCD-CT also holds potential for improved urolithiasis detection and characterization. Marcus et al. [50] showed that PCD-CT improved the detection and characterization of stones smaller than 3 mm compared to dual-energy EID-CT. These results can have clinical management implications, e.g., when an apparent single stone at EID dual-energy CT was instead shown to be two smaller stones when imaged using PCD-CT (Fig. 4d–e). Mergen

et al. have demonstrated reasonable diagnostic quality in virtual non-contrast (VNC) images relative to true non-contrast images and suggest the elimination of true non-contrast phases in the abdomen and pelvis [51].

An important consequence of multi-energy imaging is the availability of VMIs; not only can the iodine signal be increased but the CT numbers can be standardized. This may be of benefit for follow up studies, where use of the same photon-energy-level VMI can standardize the iodine enhancement, regardless of scanner make, model, or scan acquisition parameters, in addition to highlighting key imaging findings for many tasks in abdominopelvic CT due to improved iodine signal (Fig. 4f–g), similar to the use of VMIs at dual energy CT [52–55]. Because abdominopelvic CT is generally performed within a single breathhold, PCD-CT acquisition is more difficult at the thinnest collimation (120 × 0.2 mm) on the Siemens scanner, so it is generally performed with a more routine collimation (144 × 0.4 mm).

Musculoskeletal imaging

Bette et al. compared the visualization of bone details in mice specimens between PCD-CT and EID-CT [32]. In dose-matched scans, PCD-CT showed significantly lower image noise, higher bone SNR, and higher edge sharpness than EID-CT [32]. Similar results have been observed in human specimens [16; 33] and patients [16; 31] demonstrating improved visualization of cortical and trabecular architecture (Fig. 5). Some conventional EID-CT systems use dose-inefficient comb- or grid-filter based techniques for acquiring high-resolution images [56]; however, high resolution images of larger joints such as the shoulder and hips are not possible due to tube power limits and the dose penalty of these modes. With PCD-CT, ultra-high spatial resolution (e.g., 125 microns) CT images can be obtained of large body parts such as the shoulders, pelvis, and spine [31]. For smaller body parts, radiation dose will be substantially decreased owing to acquisition of images without the post-patient comb- or grid-filter [16]. The improved spatial resolution of PCD-CT has been shown to result in improved confidence in evaluation of critical anatomic strictures for large and small joints, as well as multiple myeloma lesions [16; 31; 57].

With EID dual-source CT systems, the user must choose between obtaining a high-resolution image in single-energy mode to detect subtle fractures or operating the scanner in dual-energy mode to generate virtual non-calcium images, which allow visualization of bone marrow edema that may signal an acute/subacute fracture [58]. Dual-source PCD-CT eliminates this quandary. Concurrent high spatial resolution imaging with multi-energy data is also beneficial in the work up of intraarticular and periarticular pathology with CT arthrography. With one CT acquisition, high-resolution VNC images can be generated to develop 3D bone models, without the need for a non-contrast CT arthrographic exam. PCD-CT may also be of value in the quantitative assessment of cartilage health [59] or bone mineral density [60]. Improved assessment of bone lesions has also been shown [61; 62].

Pediatric imaging

Cao at el. [63] published clinical examples of the use of PCD-CT in children, demonstrating the ability to reduce both radiation [64] and iodine doses. High pitch (e.g., 3.2) dual-source

CT for scanning of pediatric patients has previously been shown to result in acceptable image quality without the need for sedation [65]. With dual-source PCD CT, high pitch imaging can be performed for multi-energy applications, making VMIs available at energy levels selected to match the diagnostic task. One promising application of ultra-low dose CT is in the work-up of non-accidental trauma. Currently, the guidelines for the imaging work-up of non-accidental trauma set by the American College of Radiology and Society for Pediatric Radiology offer chest CT as a secondary tool when there is high clinical suspicion for abuse, but the radiographic skeletal survey is negative for fracture [66]. Fractures related to abuse can be missed on radiographs, as they are often subtle and equivocal in appearance. PCD-CT may help to detect these fractures at effective dose levels similar to a two-view chest radiograph (Supplemental Fig. 1). The use of PCD-CT to quantify cystic fibrosis in children has also been suggested [67].

Future Directions

Ultra-high-resolution imaging of the breast (e.g., breast microcalcifications)

Dedicated breast CT systems are commercially available, although their use is relatively limited at this time. One such system (nu:view; AB-CT GmbH) uses a photon counting detector [68; 69]. However, breast CT performed with whole-body CT scanners has generally not been used for diagnostic breast imaging due to limitations in spatial resolution, excessive image noise, and radiation dose considerations. With the advent of whole body PCD-CT, ultra-high-resolution breast CT imaging may be possible using whole-body systems with radiation doses similar to a chest CT exam [70]. With addition of dedicated deep learning-based CT image denoising algorithm, breast microcalcifications can be visualized (Fig. 6). The use of intravenous contrast allows assessment of iodine distribution within the breast tissue and can identify abnormal areas of breast enhancement. With the ultra-high spatial resolution mode, architectural distortion, masses, and microcalcifications can be potentially visualized at higher spatial resolution and specificity than seen on breast MR.

Quantitative CT

The ability of PCD-CT to quantify the mass densities of native tissue types and novel contrast agents based on their x-ray attenuation characteristics could enable a range of novel diagnostic and theragnostic applications. In a preclinical study, Cormode et al. [71] showed the utility of a macrophage-targeted gold-core nanoparticle (Au-HDL) to image the composition of atherosclerotic plaque in a mouse model. The authors were able to distinguish Au-HDL nanoparticles from iodine, soft tissue and calcium and confirm Au-HDL uptake in the plaque region with high macrophage activity. While dual-contrast techniques and targeted nanoparticle-based imaging using high-atomic-number contrast agents and PCD-CT are exciting, there are considerable challenges that need to be addressed before such techniques become clinically adopted. The largest barrier to clinical use is the lack of FDA-cleared high-atomic-number contrast agents other than iodine and gadolinium.

Simultaneous multi-contrast imaging

Simultaneous imaging of two or more contrast agents using one single multi-energy acquisition has been proposed for PCD-CT [47; 72–77] to generate a quantitative map of each contrast agent that corresponds to a particular physiological contrast phase. One example is to acquire bi-phase liver images in one single PCD-CT scan after sequential injection of iodine and gadolinium-based agents [73; 74]. With appropriate injection and scan timing, iodine enhancement can correspond to the late arterial phase and gadolinium enhancement can correspond to the portal-venous phase. Simultaneous imaging of iodine and gadolinium has also been proposed in biphasic kidney imaging [76], CT colonography [78], or cardiac imaging [47]. Another example is small bowel imaging using both intravascular iodine for arterial enhancement in the vascularized bowel wall and enteric bismuth for enhancement of the intestinal lumen [75]. However, the dose efficiency of simultaneous imaging of multiple contrast agents has been shown to be worse than that of a two-scan bi-phase exam due to the substantial increase in image noise from the material decomposition process [79]. This decreased dose efficiency is partially due to spectral distortions caused by many physical non-idealities of the PCD [80]. Charge summing [81], coincidence counting [82; 83], or software corrections [84; 85] for these non-ideal effects may further improve the material-specific imaging performance and improve the radiation dose efficiency. In addition, many noise reduction algorithms have been developed for material decomposition, which may also be used to control the noise and improve the quantitative results.

Summary and conclusions

PCD-CT offers numerous technical advantages over conventional EID-CT systems, fundamentally due to its different approach to x-ray detection. The promising early investigations into PCDs have led to the culmination of clinical PCD-CT systems, with high-spatial resolution, improved contrast-to-noise ratio, improved radiation dose efficiency, and the routine availability of multi-energy capabilities as notable technical features that can substantially enhance diagnostic CT. While conventional EID systems offer high spatial resolution imaging for smaller body parts, PCD-CT extends this benefit to all body parts and across a range of diagnostic tasks. Similarly, the benefits of multi-energy imaging can now be combined with dual-source high temporal resolution and high pitch imaging. High spatial resolution combined with multi-energy imaging at PCD-CT can be used to reduce calcium bloom and metallic artifacts, which often limit diagnostic assessment. We anticipate that in coming years, the improved visualization of key anatomic features, reduction of artifacts, and simultaneous multi-energy capabilities will result in improved clinical outcomes for specific diagnostic tasks. The improved diagnostic information available with higher spatial resolution at lower radiation doses is expected to expand the information provided by these exams and result in new types of exams performed routinely with CT.

Supplementary Material

Refer to Web version on PubMed Central for supplementary material.

Abbreviations:

PCD	photon counting detector
EID	energy integrating detector
SNR	signal to noise ratio
CTA	CT angiography
VMI	virtual monoenergetic image
VNC	virtual non-contrast
ILD	Interstitial lung disease

References:

1. McCollough C, Rajendran K, Leng S et al. (2022) The technical development of photon counting detector CT. Euro Radiol In Press
2. Benjaminov O, Perlow E, Romman Z et al. (2008) Novel, Energy-Discriminating Photon Counting CT System (EDCT): First Clinical Evaluation—CT Angiography: Carotid Artery StenosisRadiological Society of North America 2008 Scientific Assembly and Annual Meeting, Chicago, Il.
3. Leng S, Rajendran K, Gong H et al. (2018) 150-μm Spatial Resolution Using Photon-Counting Detector Computed Tomography Technology: Technical Performance and First Patient Images. Invest Radiol 53:655–662 [PubMed: 29847412]
4. Pourmorteza A, Symons R, Sandfort V et al. (2016) Abdominal Imaging with Contrast-enhanced Photon-counting CT: First Human Experience. Radiology 279:239–245 [PubMed: 26840654]
5. Yu Z, Leng S, Jorgensen SM et al. (2016) Evaluation of conventional imaging performance in a research whole-body CT system with a photon-counting detector array. Phys Med Biol 61:1572–1595 [PubMed: 26835839]
6. Si-Mohamed S, Bar-Ness D, Sigovan M et al. (2017) Review of an initial experience with an experimental spectral photon-counting computed tomography system. Nuclear Instruments & Methods in Physics Research Section a-Accelerators Spectrometers Detectors and Associated Equipment 873:27–35
7. Ferda J, Vendis T, Flohr T et al. (2021) Computed tomography with a full FOV photon-counting detector in a clinical setting, the first experience. Eur J Radiol 137:109614 [PubMed: 33657475]
8. Rajendran K, Petersilka M, Henning A et al. (2021) Full field-of-view, high-resolution, photon-counting detector CT: technical assessment and initial patient experience. Phys Med Biol 66
9. Rajendran K, Petersilka M, Henning A et al. (2022) First Clinical Photon-counting Detector CT System: Technical Evaluation. Radiology 303:130–138 [PubMed: 34904876]
10. Yu Z, Leng S, Kappler S et al. (2016) Noise performance of low-dose CT: comparison between an energy integrating detector and a photon counting detector using a whole-body research photon counting CT scanner. J Med Imaging (Bellingham) 3:043503 [PubMed: 28018936]
11. Symons R, Cork TE, Sahbaee P et al. (2017) Low-dose lung cancer screening with photon-counting CT: a feasibility study. Phys Med Biol 62:202–213 [PubMed: 27991453]
12. Symons R, Pourmorteza A, Sandfort V et al. (2017) Feasibility of Dose-reduced Chest CT with Photon-counting Detectors: Initial Results in Humans. Radiology 285:980–989 [PubMed: 28753389]
13. Leng S, Bruesewitz M, Tao S et al. (2019) Photon-counting Detector CT: System Design and Clinical Applications of an Emerging Technology. RadioGraphics 39:729–743 [PubMed: 31059394]

14. Hagen F, Walder L, Fritz J et al. (2022) Image Quality and Radiation Dose of Contrast-Enhanced Chest-CT Acquired on a Clinical Photon-Counting Detector CT vs. Second-Generation Dual-Source CT in an Oncologic Cohort: Preliminary Results. Tomography 8:1466–1476 [PubMed: 35736867]
15. Jungblut L, Euler A, von Spiczak J et al. (2022) Potential of Photon-Counting Detector CT for Radiation Dose Reduction for the Assessment of Interstitial Lung Disease in Patients With Systemic Sclerosis. Invest Radiol. 10.1097/RLI.0000000000000895
16. Rajendran K, Baffour F, Powell G et al. (2022) Improved visualization of the wrist at lower radiation dose with photon-counting-detector CT. Skeletal Radiol. 10.1007/s00256-022-04117-2
17. Rajendran K, Voss BA, Zhou W et al. (2020) Dose Reduction for Sinus and Temporal Bone Imaging Using Photon-Counting Detector CT With an Additional Tin Filter. Invest Radiol 55:91–100 [PubMed: 31770297]
18. Zhou W, Bartlett DJ, Diehn FE et al. (2019) Reduction of Metal Artifacts and Improvement in Dose Efficiency Using Photon-Counting Detector Computed Tomography and Tin Filtration. Invest Radiol 54:204–211 [PubMed: 30562270]
19. Sawall S, Klein L, Amato C et al. (2020) Iodine contrast-to-noise ratio improvement at unit dose and contrast media volume reduction in whole-body photon-counting CT. Eur J Radiol 126:108909 [PubMed: 32145600]
20. Euler A, Higashigaito K, Mergen V et al. (2022) High-Pitch Photon-Counting Detector Computed Tomography Angiography of the Aorta: Intraindividual Comparison to Energy-Integrating Detector Computed Tomography at Equal Radiation Dose. Invest Radiol 57:115–121 [PubMed: 34352805]
21. Harvey EC, Feng M, Ji X et al. (2019) Impacts of photon counting CT to maximum intensity projection (MIP) images of cerebral CT angiography: theoretical and experimental studies. Phys Med Biol 64:185015 [PubMed: 31315093]
22. Symons R, Reich DS, Bagheri M et al. (2018) Photon-Counting Computed Tomography for Vascular Imaging of the Head and Neck: First In Vivo Human Results. Invest Radiol 53:135–142 [PubMed: 28926370]
23. Benson JC, Rajendran K, Lane JI et al. (2022) A New Frontier in Temporal Bone Imaging: Photon-Counting Detector CT Demonstrates Superior Visualization of Critical Anatomic Structures at Reduced Radiation Dose. AJNR Am J Neuroradiol 43:579–584 [PubMed: 35332019]
24. Zhou W, Lane JI, Carlson ML et al. (2018) Comparison of a Photon-Counting-Detector CT with an Energy-Integrating-Detector CT for Temporal Bone Imaging: A Cadaveric Study. AJNR Am J Neuroradiol 39:1733–1738 [PubMed: 30093479]
25. Si-Mohamed S, Boccalini S, Rodesch PA et al. (2021) Feasibility of lung imaging with a large field-of-view spectral photon-counting CT system. Diagn Interv Imaging 102:305–312 [PubMed: 33610503]
26. Bartlett DJ, Koo CW, Bartholmai BJ et al. (2019) High-Resolution Chest Computed Tomography Imaging of the Lungs: Impact of 1024 Matrix Reconstruction and Photon-Counting Detector Computed Tomography. Invest Radiol 54:129–137 [PubMed: 30461437]
27. Mergen V, Sartoretti T, Baer-Beck M et al. (2022) Ultra-High-Resolution Coronary CT Angiography With Photon-Counting Detector CT: Feasibility and Image Characterization. Invest Radiol. 10.1097/RLI.0000000000000897
28. Si-Mohamed SA, Boccalini S, Lacombe H et al. (2022) Coronary CT Angiography with Photon-counting CT: First-In-Human Results. Radiology 303:303–313 [PubMed: 35166583]
29. Sandstedt M, Marsh J Jr., Rajendran K et al. (2021) Improved coronary calcification quantification using photon-counting-detector CT: an ex vivo study in cadaveric specimens. Eur Radiol 31:6621–6630 [PubMed: 33713174]
30. Symons R, De Bruecker Y, Roosen J et al. (2018) Quarter-millimeter spectral coronary stent imaging with photon-counting CT: Initial experience. J Cardiovasc Comput Tomogr 12:509–515 [PubMed: 30509378]
31. Baffour FI, Rajendran K, Glazebrook KN et al. (2022) Ultra-high-resolution imaging of the shoulder and pelvis using photon-counting-detector CT: a feasibility study in patients. Eur Radiol. 10.1007/s00330-022-08925-x

32. Bette SJ, Braun FM, Haerting M et al. (2022) Visualization of bone details in a novel photon-counting dual-source CT scanner-comparison with energy-integrating CT. Eur Radiol 32:2930–2936 [PubMed: 34936011]
33. Klintström B, Henriksson L, Moreno R et al. (2022) Photon-counting detector CT and energy-integrating detector CT for trabecular bone microstructure analysis of cubic specimens from human radius. Eur Radiol Exp 6:31 [PubMed: 35882679]
34. McCollough CH, Boedeker K, Cody D et al. (2020) Principles and applications of multienergy CT: Report of AAPM Task Group 291. Medical Physics 47:e881–e912 [PubMed: 32215937]
35. McCollough CH, Leng S, Yu L, Fletcher JG (2015) Dual- and Multi-Energy CT: Principles, Technical Approaches, and Clinical Applications. Radiology 276:637–653 [PubMed: 26302388]
36. Tao A, Huang R, Tao S, Michalak GJ, McCollough CH, Leng S (2019) Dual-source photon counting detector CT with a tin filter: a phantom study on iodine quantification performance. Phys Med Biol 64:115019 [PubMed: 31018197]
37. Sartoretti T, Mergen V, Jungblut L, Alkadhi H, Euler A (2022) Liver Iodine Quantification With Photon-Counting Detector CT: Accuracy in an Abdominal Phantom and Feasibility in Patients. Acad Radiol. 10.1016/j.acra.2022.04.021
38. Roessl E, Proksa R (2007) K-edge imaging in x-ray computed tomography using multi-bin photon counting detectors. Phys Med Biol 52:4679–4696 [PubMed: 17634657]
39. Do TD, Sawall S, Heinze S et al. (2020) A semi-automated quantitative comparison of metal artifact reduction in photon-counting computed tomography by energy-selective thresholding. Scientific Reports 10:21099 [PubMed: 33273590]
40. Long Z, DeLone DR, Kotsenas AL et al. (2019) Clinical Assessment of Metal Artifact Reduction Methods in Dual-Energy CT Examinations of Instrumented Spines. AJR Am J Roentgenol 212:395–401 [PubMed: 30667317]
41. Campeau NG, Farnsworth PJ, Diehn FE et al. (2022) High resolution CTA of the Orbit Using a Photon Counting CT scanner 108th Scientific Assembly and Annual Meeting. Radiological Society of North America (RSNA), Chicago, IL
42. Inoue A, Johnson TF, White D et al. (2022) Estimating the Clinical Impact of Photon-Counting-Detector CT in Diagnosing Usual Interstitial Pneumonia. Investigative Radiology. 10.1097/rli.0000000000000888:10.1097/RLI.0000000000000888
43. Lu GM, Zhao Y, Zhang LJ, Schoepf UJ (2012) Dual-energy CT of the lung. AJR Am J Roentgenol 199:S40–53 [PubMed: 23097167]
44. Sandfort V, Persson M, Pourmorteza A, Noel PB, Fleischmann D, Willemink MJ (2021) Spectral photon-counting CT in cardiovascular imaging. J Cardiovasc Comput Tomogr 15:218–225 [PubMed: 33358186]
45. Allmendinger T, Nowak T, Flohr T et al. (2022) Photon-Counting Detector CT-Based Vascular Calcium Removal Algorithm: Assessment Using a Cardiac Motion Phantom. Invest Radiol 57:399–405 [PubMed: 35025834]
46. Kalisz K, Halliburton S, Abbara S et al. (2017) Update on Cardiovascular Applications of Multienergy CT. RadioGraphics 37:1955–1974 [PubMed: 29131773]
47. Symons R, Cork TE, Lakshmanan MN et al. (2017) Dual-contrast agent photon-counting computed tomography of the heart: initial experience. Int J Cardiovasc Imaging 33:1253–1261 [PubMed: 28289990]
48. Decker JA, Bette S, Lubina N et al. (2022) Low-dose CT of the abdomen: Initial experience on a novel photon-counting detector CT and comparison with energy-integrating detector CT. Eur J Radiol 148:110181 [PubMed: 35121331]
49. Higashigaito K, Euler A, Eberhard M, Flohr TG, Schmidt B, Alkadhi H (2022) Contrast-Enhanced Abdominal CT with Clinical Photon-Counting Detector CT: Assessment of Image Quality and Comparison with Energy-Integrating Detector CT. Acad Radiol 29:689–697 [PubMed: 34389259]
50. Marcus RP, Fletcher JG, Ferrero A et al. (2018) Detection and Characterization of Renal Stones by Using Photon-Counting-based CT. Radiology 289:436–442 [PubMed: 30084728]
51. Mergen V, Racine D, Jungblut L et al. (2022) Virtual Noncontrast Abdominal Imaging with Photon-counting Detector CT. Radiology. 10.1148/radiol.213260:213260

52. Leng S, Zhou W, Yu Z et al. (2017) Spectral performance of a whole-body research photon counting detector CT: quantitative accuracy in derived image sets. Phys Med Biol 62:7216–7232 [PubMed: 28726669]
53. Michalak G, Grimes J, Fletcher J et al. (2016) Technical Note: Improved CT number stability across patient size using dual-energy CT virtual monoenergetic imaging. Med Phys 43:513 [PubMed: 26745944]
54. Voss BA, Khandelwal A, Wells ML et al. (2022) Impact of dual-energy 50-keV virtual monoenergetic images on radiologist confidence in detection of key imaging findings of small hepatocellular carcinomas using multiphase liver CT. Acta Radiol 63:1443–1452 [PubMed: 34723681]
55. Zhou W, Michalak GJ, Weaver JM et al. (2020) A Universal Protocol for Abdominal CT Examinations Performed on a Photon-Counting Detector CT System: A Feasibility Study. Invest Radiol 55:226–232 [PubMed: 32049691]
56. Flohr TG, Stierstorfer K, Suss C, Schmidt B, Primak AN, McCollough CH (2007) Novel ultrahigh resolution data acquisition and image reconstruction for multi-detector row CT. Med Phys 34:1712–1723 [PubMed: 17555253]
57. Baffour FI, Huber NR, Ferrero A et al. (2022) Photon-counting Detector CT with Deep Learning Noise Reduction to Detect Multiple Myeloma. Radiology. 10.1148/radiol.220311:220311
58. Gosangi B, Mandell JC, Weaver MJ et al. (2020) Bone Marrow Edema at Dual-Energy CT: A Game Changer in the Emergency Department. RadioGraphics 40:859–874 [PubMed: 32364883]
59. Rajendran K, Löbker C, Schon BS et al. (2017) Quantitative imaging of excised osteoarthritic cartilage using spectral CT. Eur Radiol 27:384–392 [PubMed: 27165137]
60. Nowak T, Eberhard M, Schmidt B et al. (2021) Bone Mineral Density Quantification from Localizer Radiographs: Accuracy and Precision of Energy-integrating Detector CT and Photon-counting Detector CT. Radiology 298:147–152 [PubMed: 33141002]
61. Huber N, Anderson T, Missert A et al. (2022) Clinical evaluation of a phantom-based deep convolutional neural network for whole-body-low-dose and ultra-low-dose CT skeletal surveys. Skeletal Radiol 51:145–151 [PubMed: 34114078]
62. Wehrse E, Sawall S, Klein L et al. (2021) Potential of ultra-high-resolution photon-counting CT of bone metastases: initial experiences in breast cancer patients. NPJ Breast Cancer 7:3 [PubMed: 33398008]
63. Cao J, Bache S, Schwartz FR, Frush D (2022) Pediatric Applications of Photon-Counting Detector CT. AJR Am J Roentgenol. 10.2214/ajr.22.28391
64. Wang X, Zamyatin A, Shi D (2012) Dose reduction potential with photon counting computed tomographyMedical Imaging 2012: Physics of Medical Imaging. SPIE, San Diego, California, United States, pp 1193–1198
65. Kino A, Zucker EJ, Honkanen A et al. (2019) Ultrafast pediatric chest computed tomography: comparison of free-breathing vs. breath-hold imaging with and without anesthesia in young children. Pediatr Radiol 49:301–307 [PubMed: 30413857]
66. Wootton-Gorges SL, Soares BP, Alazraki AL et al. (2017) ACR Appropriateness Criteria(®) Suspected Physical Abuse-Child. J Am Coll Radiol 14:S338–s349 [PubMed: 28473090]
67. Horst K, Hull N, Thacker P et al. (2022) Pilot Study to Determine if Reduced-dose Photon Counting Detector (PCD) Chest CT Can Reliably Display Brody II Score Imaging Findings for Children with Cystic Fibrosis at Radiation Doses that Approximate Radiographs. Pediatr Radiol In Press
68. Berger N, Marcon M, Frauenfelder T, Boss A (2020) Dedicated Spiral Breast Computed Tomography With a Single Photon-Counting Detector: Initial Results of the First 300 Women. Invest Radiol 55:68–72 [PubMed: 31592797]
69. Berger N, Marcon M, Saltybaeva N et al. (2019) Dedicated Breast Computed Tomography With a Photon-Counting Detector: Initial Results of Clinical In Vivo Imaging. Invest Radiol 54:409–418 [PubMed: 30829942]
70. Huber NR, Ferrero A, Rajendran K et al. (2022) Dedicated convolutional neural network for noise reduction in ultra-high-resolution photon-counting detector computed tomography. Physics in Medicine & Biology

71. Cormode DP, Roessl E, Thran A et al. (2010) Atherosclerotic plaque composition: analysis with multicolor CT and targeted gold nanoparticles. Radiology 256:774–782 [PubMed: 20668118]
72. Cormode DP, Si-Mohamed S, Bar-Ness D et al. (2017) Multicolor spectral photon-counting computed tomography: in vivo dual contrast imaging with a high count rate scanner. Sci Rep 7:4784 [PubMed: 28684756]
73. Muenzel D, Daerr H, Proksa R et al. (2017) Simultaneous dual-contrast multi-phase liver imaging using spectral photon-counting computed tomography: a proof-of-concept study. Eur Radiol Exp 1:25 [PubMed: 29708205]
74. Ren L, Huber N, Rajendran K, Fletcher JG, McCollough CH, Yu L (2022) Dual-Contrast Biphasic Liver Imaging With Iodine and Gadolinium Using Photon-Counting Detector Computed Tomography: An Exploratory Animal Study. Invest Radiol 57:122–129 [PubMed: 34411033]
75. Ren L, Rajendran K, Fletcher JG, McCollough CH, Yu L (2020) Simultaneous Dual-Contrast Imaging of Small Bowel With Iodine and Bismuth Using Photon-Counting-Detector Computed Tomography: A Feasibility Animal Study. Invest Radiol 55:688–694 [PubMed: 32530868]
76. Symons R, Krauss B, Sahbaee P et al. (2017) Photon-counting CT for simultaneous imaging of multiple contrast agents in the abdomen: An in vivo study. Med Phys 44:5120–5127 [PubMed: 28444761]
77. Tao S, Rajendran K, McCollough CH, Leng S (2019) Feasibility of multi-contrast imaging on dual-source photon counting detector (PCD) CT: An initial phantom study. Med Phys 46:4105–4115 [PubMed: 31215659]
78. Muenzel D, Bar-Ness D, Roessl E et al. (2017) Spectral Photon-counting CT: Initial Experience with Dual-Contrast Agent K-Edge Colonography. Radiology 283:723–728 [PubMed: 27918709]
79. Ren L, Rajendran K, McCollough CH, Yu L (2019) Radiation dose efficiency of multi-energy photon-counting-detector CT for dual-contrast imaging. Phys Med Biol 64:245003 [PubMed: 31703217]
80. Taguchi K, Iwanczyk JS (2013) Vision 20/20: Single photon counting x-ray detectors in medical imaging. Med Phys 40:100901 [PubMed: 24089889]
81. Ballabriga R, Campbell M, Heijne EHM, Llopart X, Tlustos L (2007) The Medipix3 Prototype, a Pixel Readout Chip Working in Single Photon Counting Mode With Improved Spectrometric Performance. IEEE Transactions on Nuclear Science 54:1824–1829
82. Hsieh SS (2020) Coincidence Counters for Charge Sharing Compensation in Spectroscopic Photon Counting Detectors. IEEE Trans Med Imaging 39:678–687 [PubMed: 31398114]
83. Hsieh SS, Sjolin M (2018) Digital count summing vs analog charge summing for photon counting detectors: A performance simulation study. Med Phys. 10.1002/mp.13098
84. Blaj G (2019) Dead-time correction for spectroscopic photon-counting pixel detectors. J Synchrotron Radiat 26:1621–1630 [PubMed: 31490152]
85. Touch M, Clark DP, Barber W, Badea CT (2016) A neural network-based method for spectral distortion correction in photon counting x-ray CT. Phys Med Biol 61:6132–6153 [PubMed: 27469292]

Key points:

1. Beneficial characteristics of photon-counting detectors include absence of electronic noise, increased iodine signal-to-noise-ratio, improved spatial resolution, and full-time multi-energy imaging.
2. Promising applications of PCD-CT involve imaging of anatomy where exquisite spatial resolution adds clinical value and applications requiring multi-energy data simultaneous with high spatial and/or temporal resolution.
3. Future applications of PCD-CT technology may include extremely high spatial resolution tasks, such as detection of breast micro-calcifications, and quantitative imaging of native tissue types and novel contrast agents.

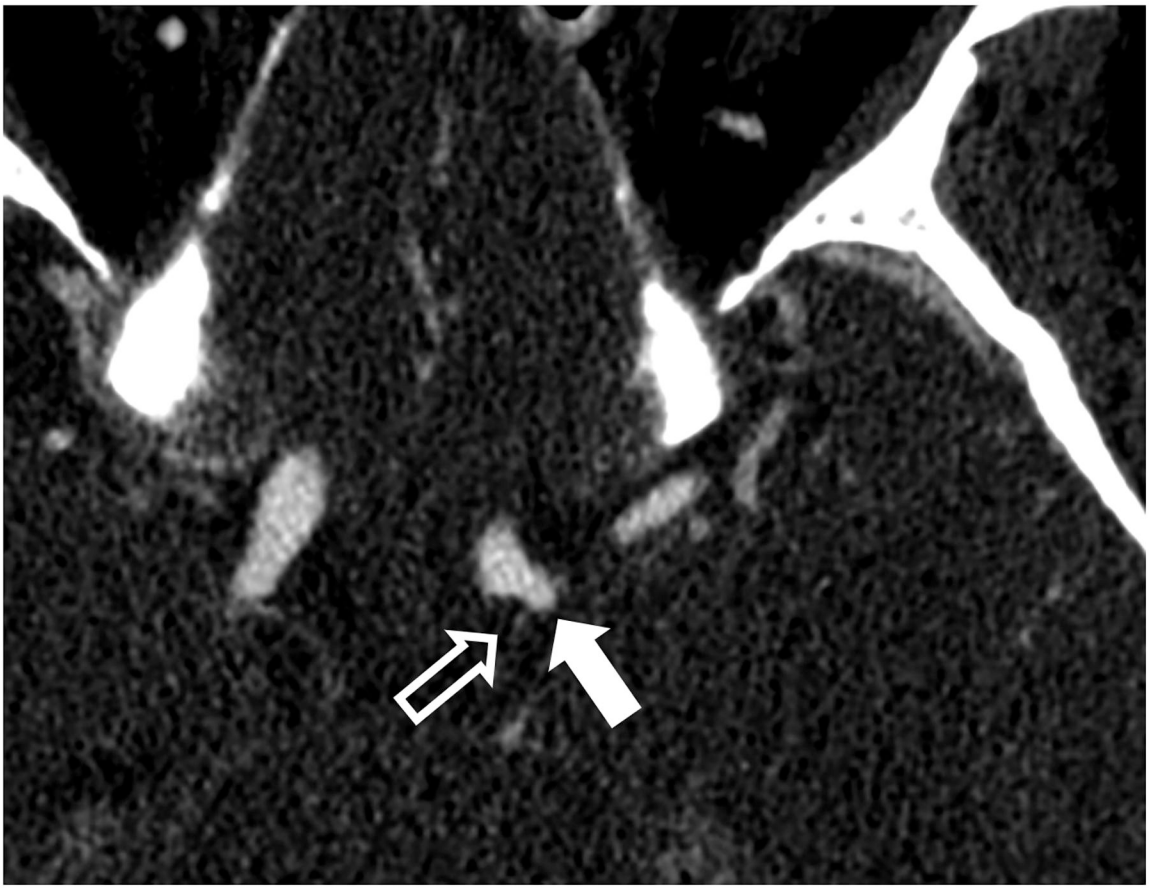

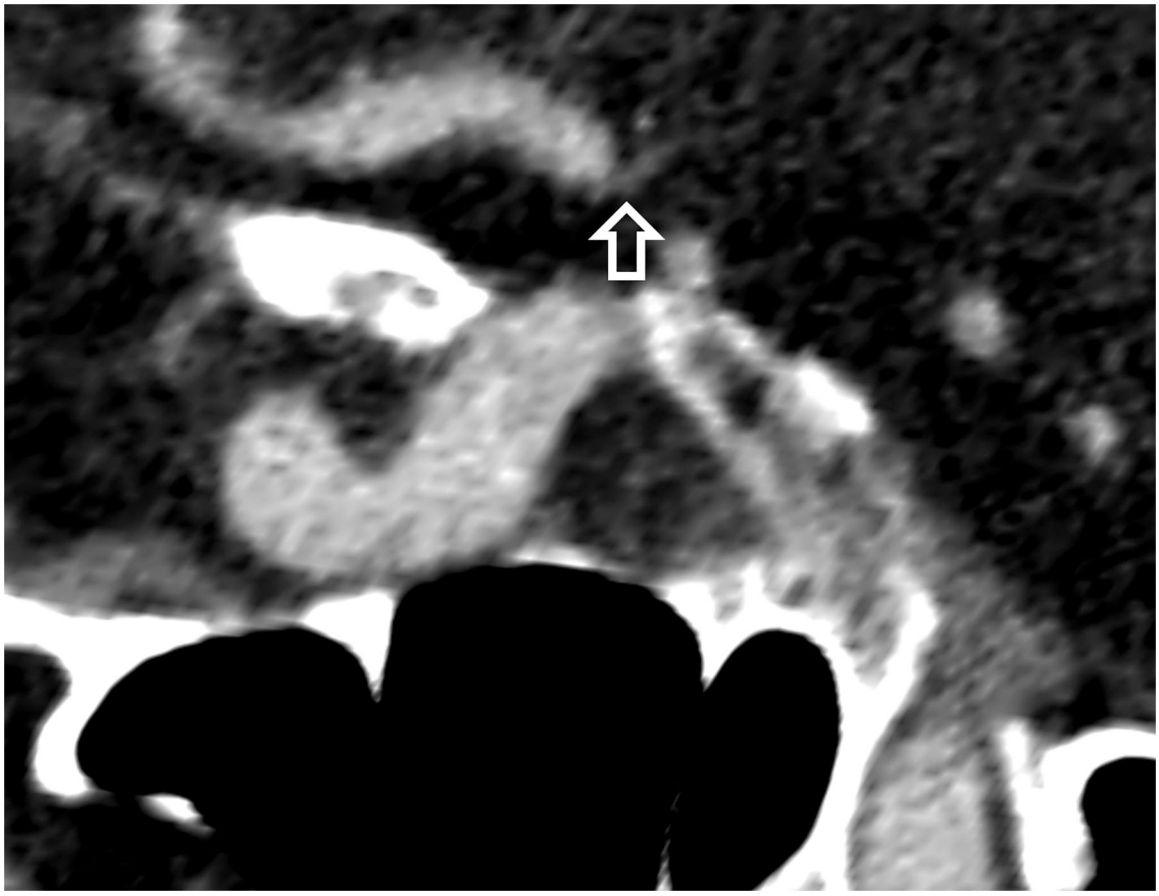

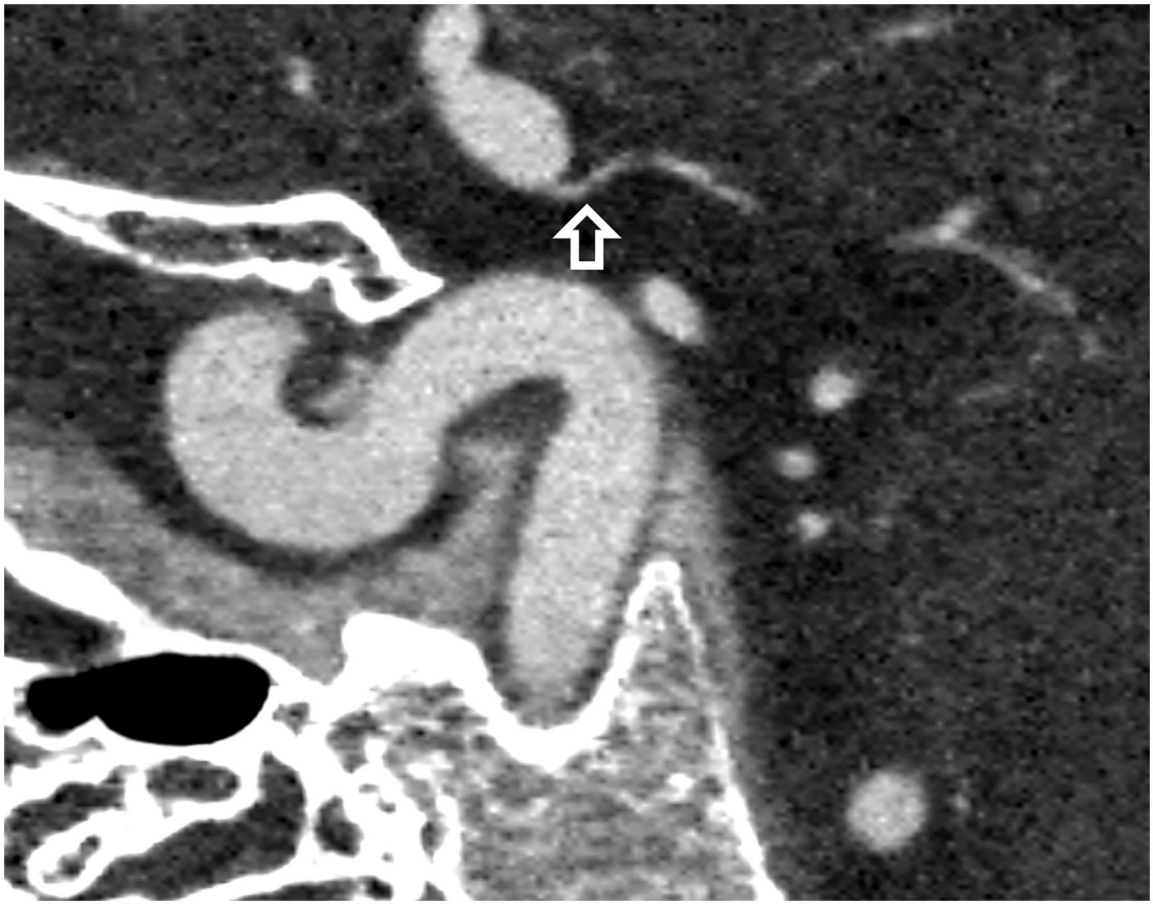

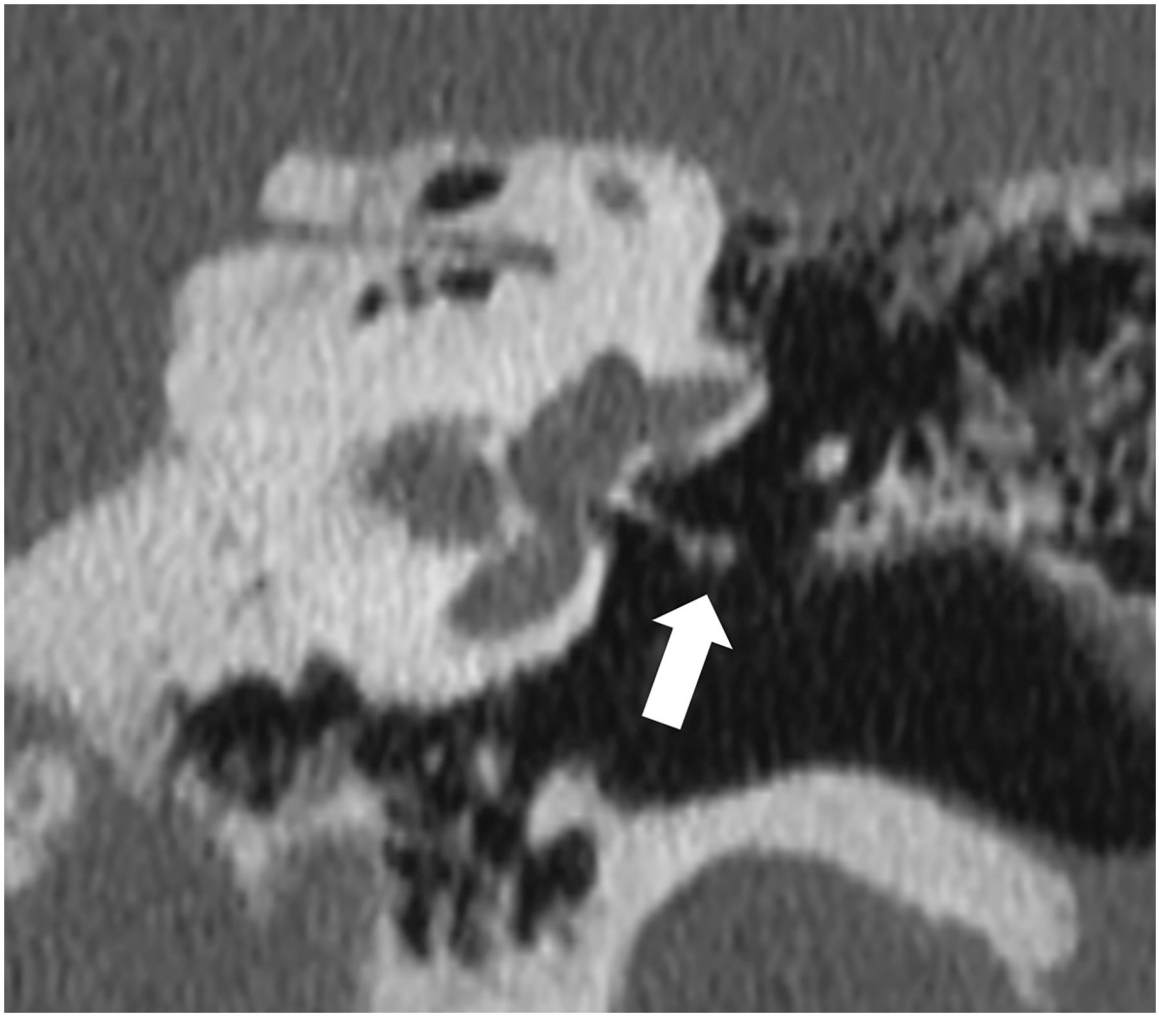

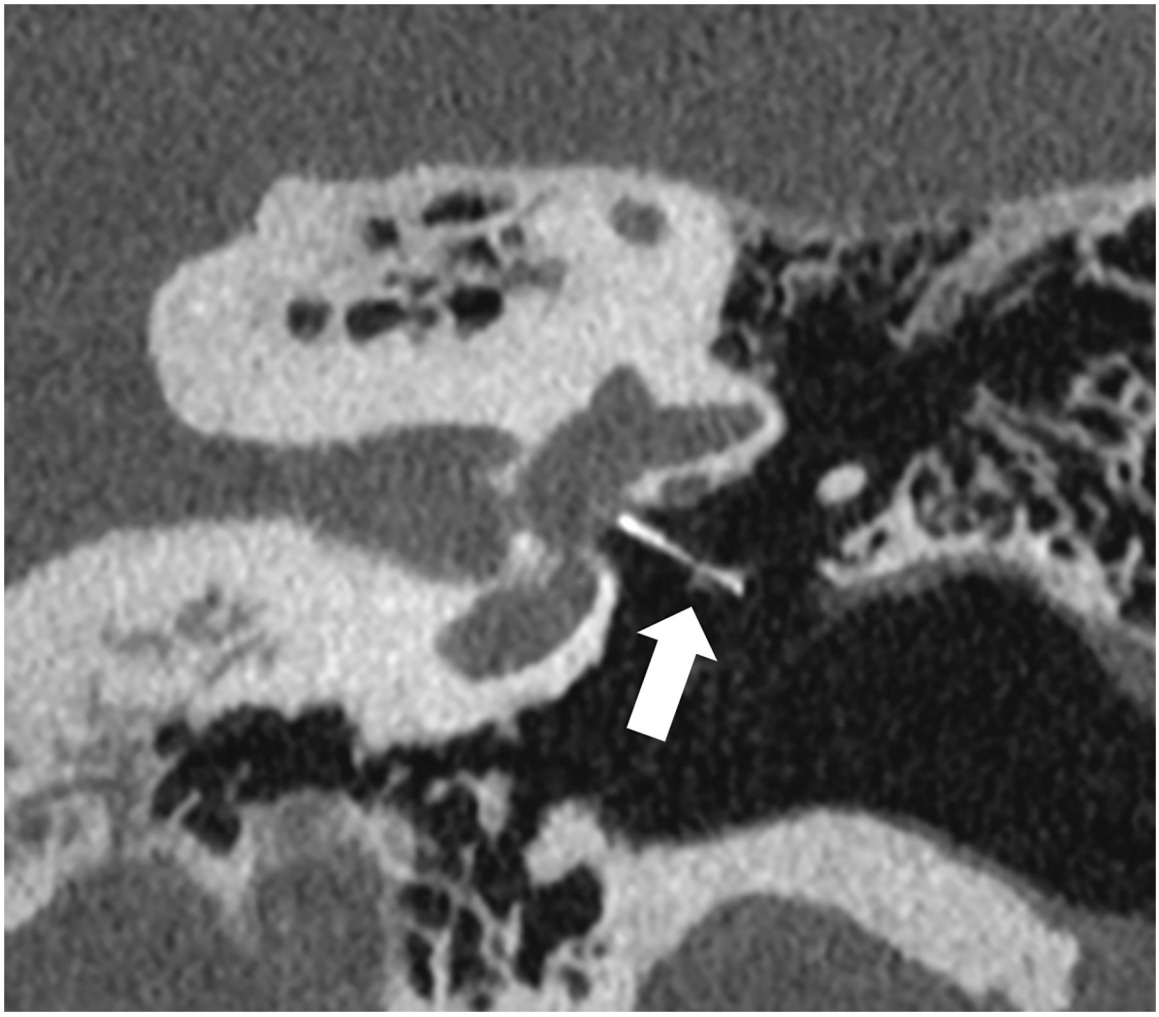

Figure 1:
Thin section axial and oblique sagittal head CTA images of a 61-year-old male, using EID with 0.6-mm slice thickness (A-B, top row) and PCD-CT (120 kV PCD image comprising 20–120 keV photons) with high resolution mode including 0.2-mm slice thickness (C-D, bottom row) techniques. An ~2-mm left supraclinoid ICA outpouching (infundibulum vs. aneurysm) is seen on EID (solid white arrow in A), but better delineated on PCD (solid white arrow in C). Specifically, the small vessel (anterior choroidal artery) arising from the apex of the outpouching is much better visualized on PCD (open arrows in C-D) than EID (open arrows in A-B), confirming an infundibulum rather than an aneurysm. In a 53-year-old male patient undergoing temporal bone imaging at EID-CT (E) and PCD-CT (120 kV PCD image comprising 20–120 keV photons, F), a stapes prosthesis (solid white arrow) is much better delineated on oblique coronal images using PCD with 0.2-mm slice thickness (F) than EID-CT with 0.4-mm slice thickness (E); the radiation dose was lower for PCD than EID (36 vs. 56 mGy, respectively). E and F reproduced with permission from [23]. [EID: energy integrating detector; PCD: photon-counting-detector]

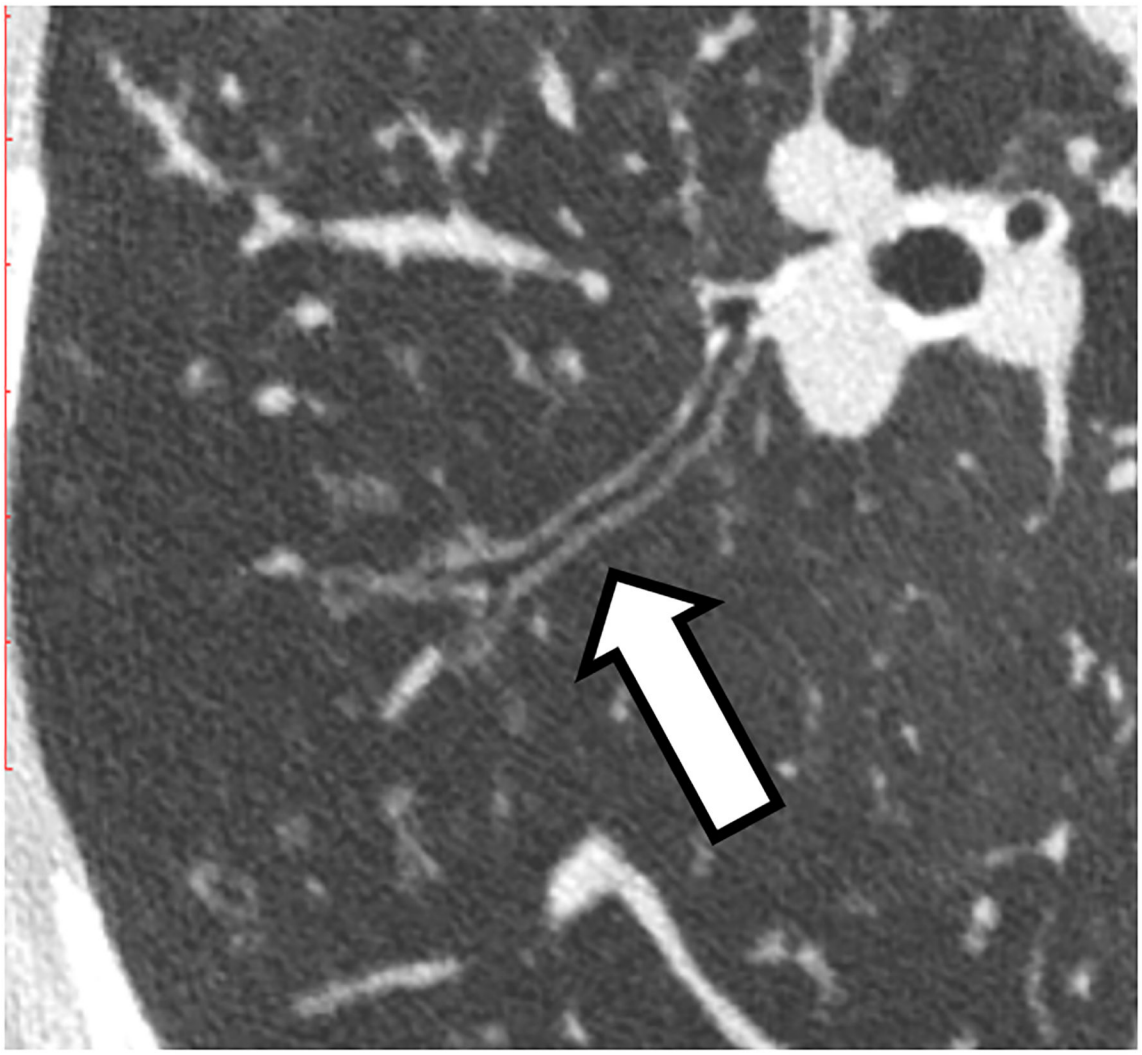

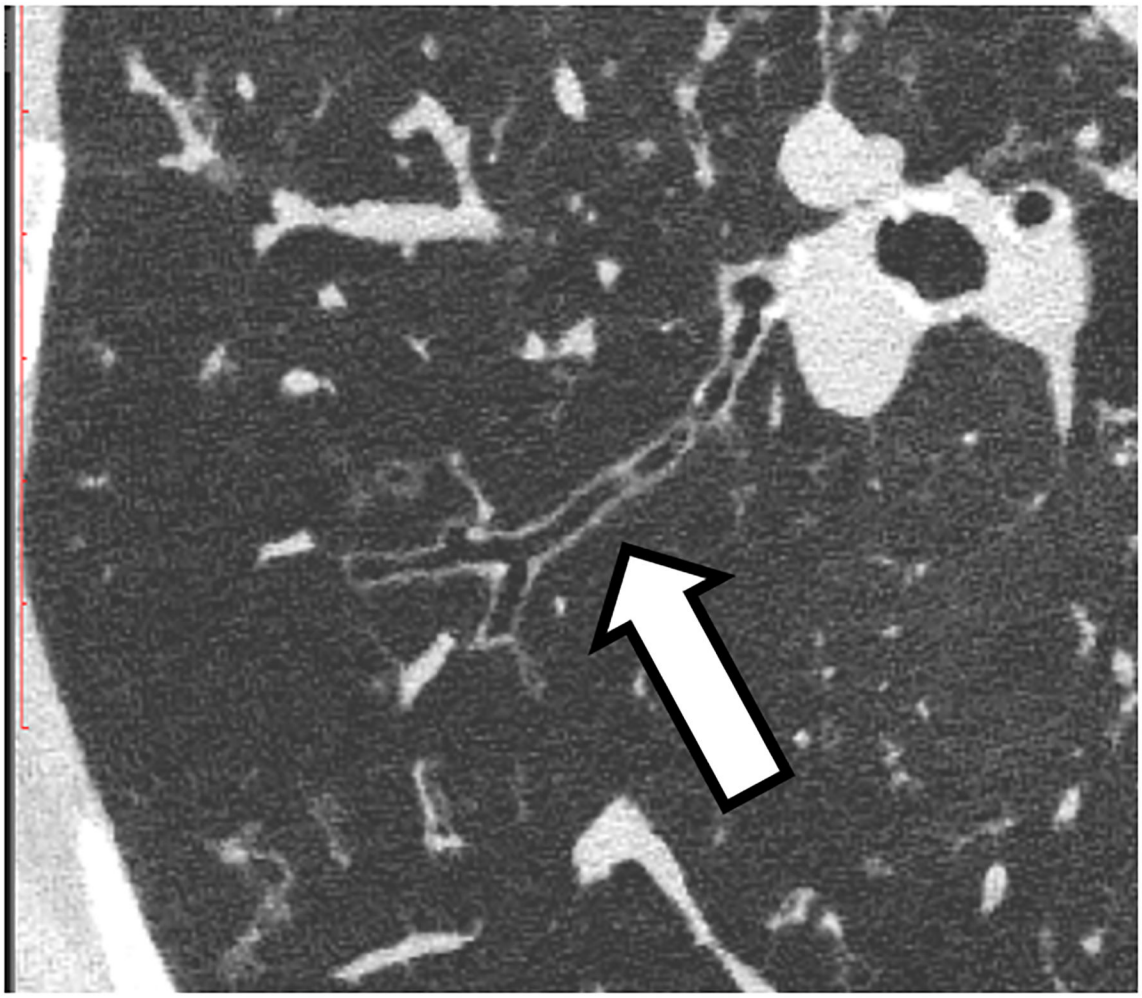

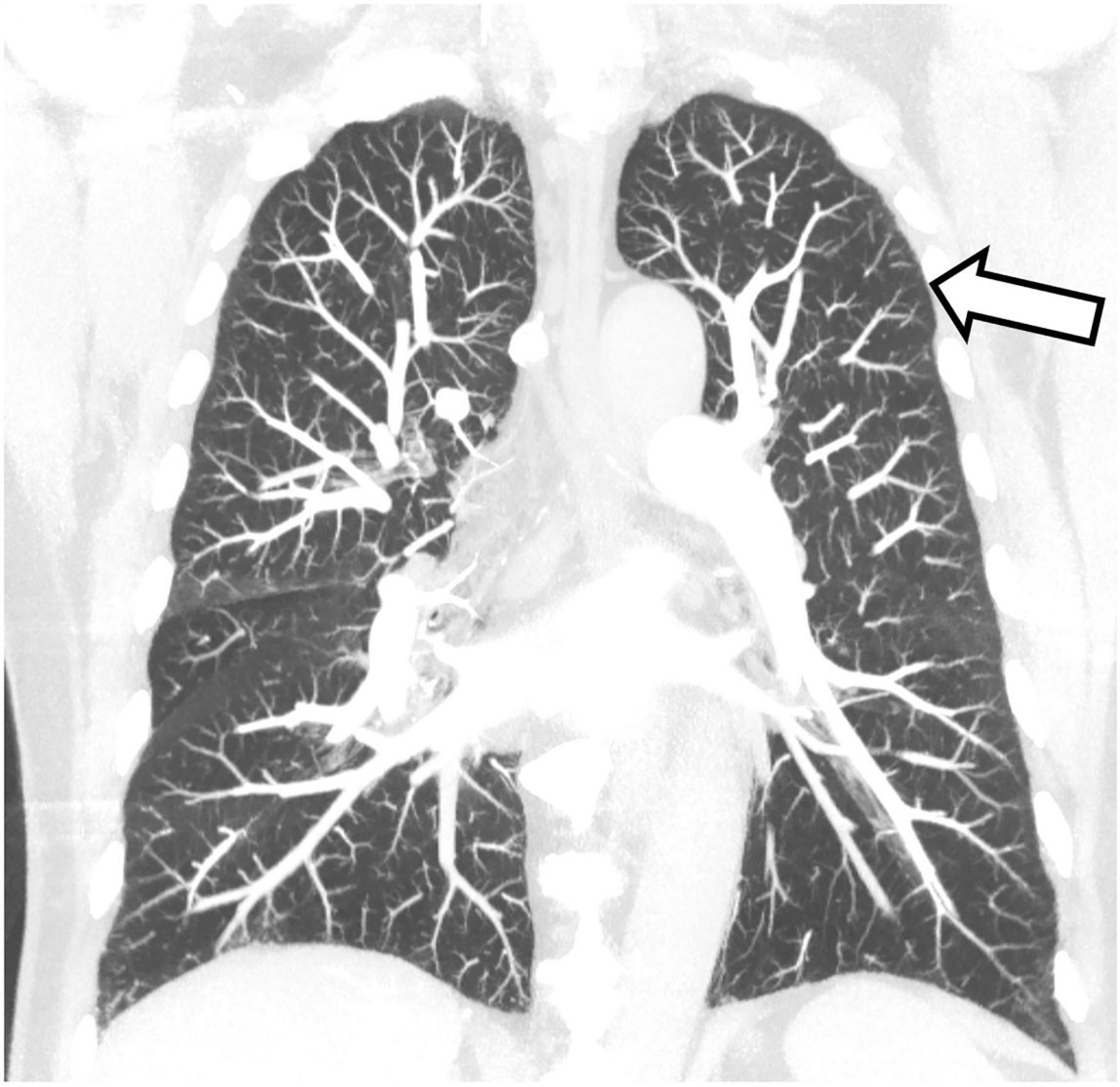

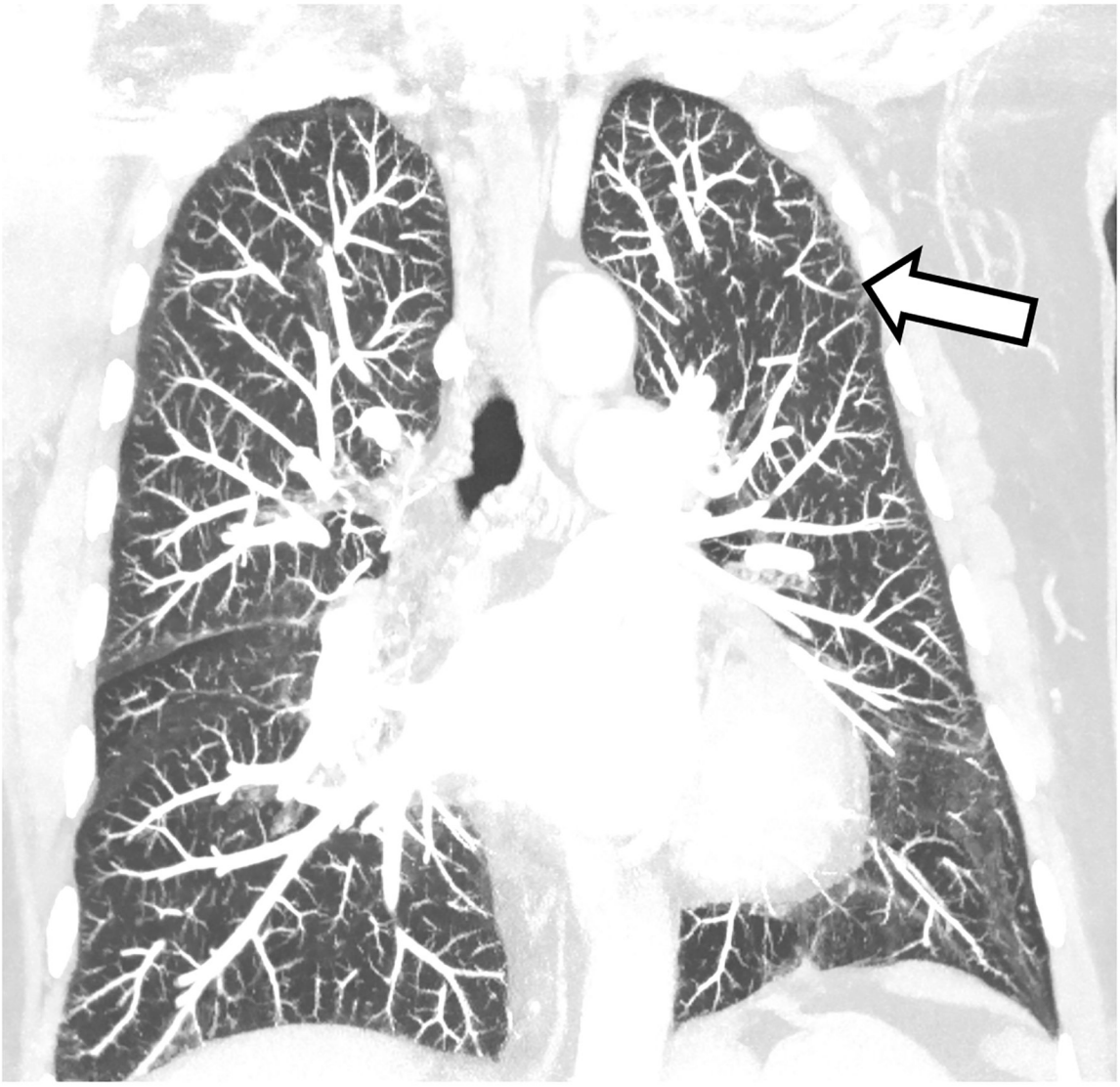

Figure 2:
Improved visualization of bronchial walls relative to EID-CT (A) are seen with PCD-CT (B) in these non-enhanced chest CT images of a 70-year-old female. In EID-CT (C) and PCD-CT (D) images from a contrast-enhanced chest CT of a 77-year-old male, the improved spatial resolution and iodine signal of PCD-CT allows the increased sharpness of the vascular tree to extend right to the periphery of the lung. PCD-CT images obtained at 120 kV and comprise 20–120 keV photons. A and B reproduced with permission from [8]. [EID: energy integrating detector; PCD: photon-counting-detector]

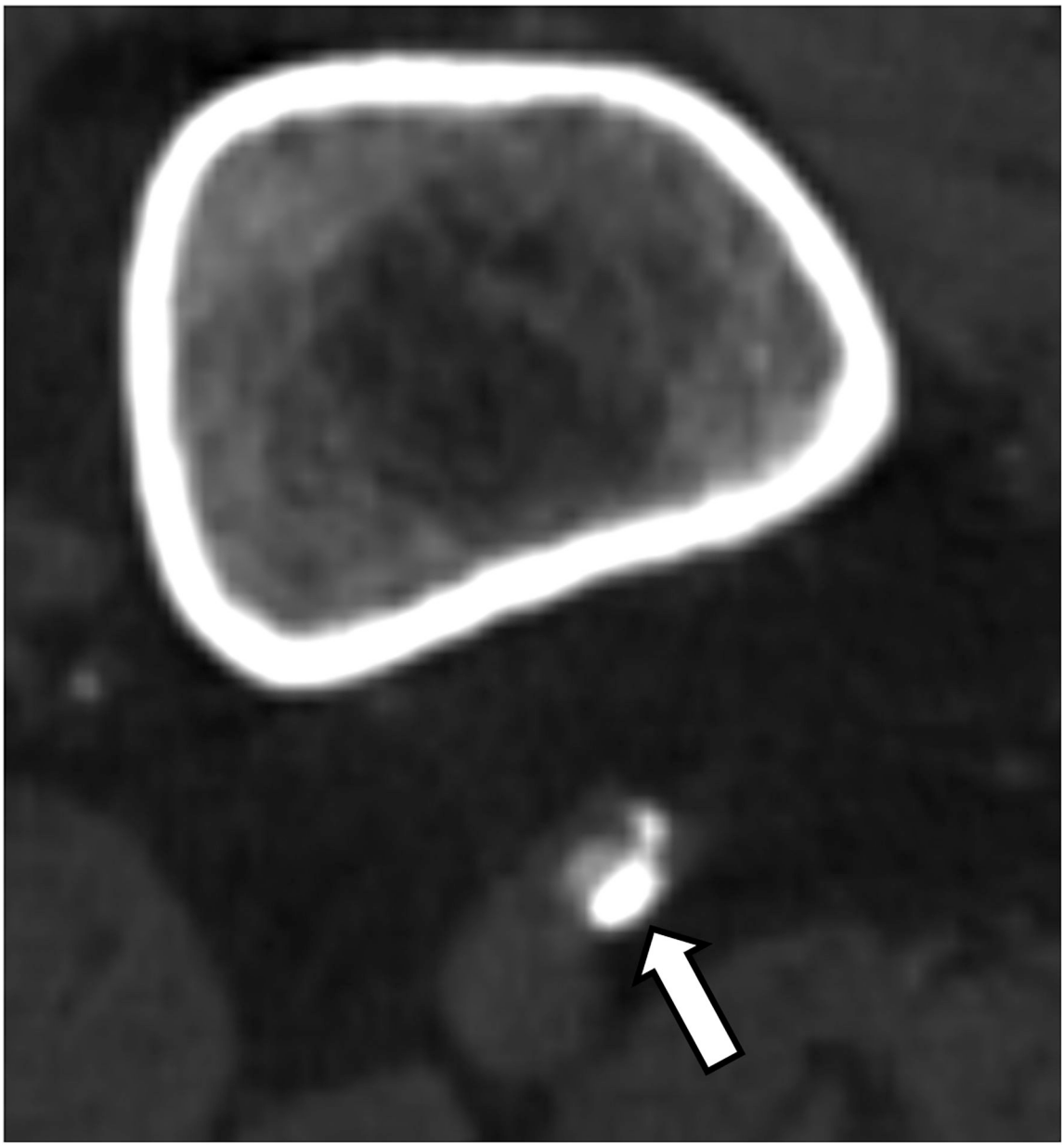

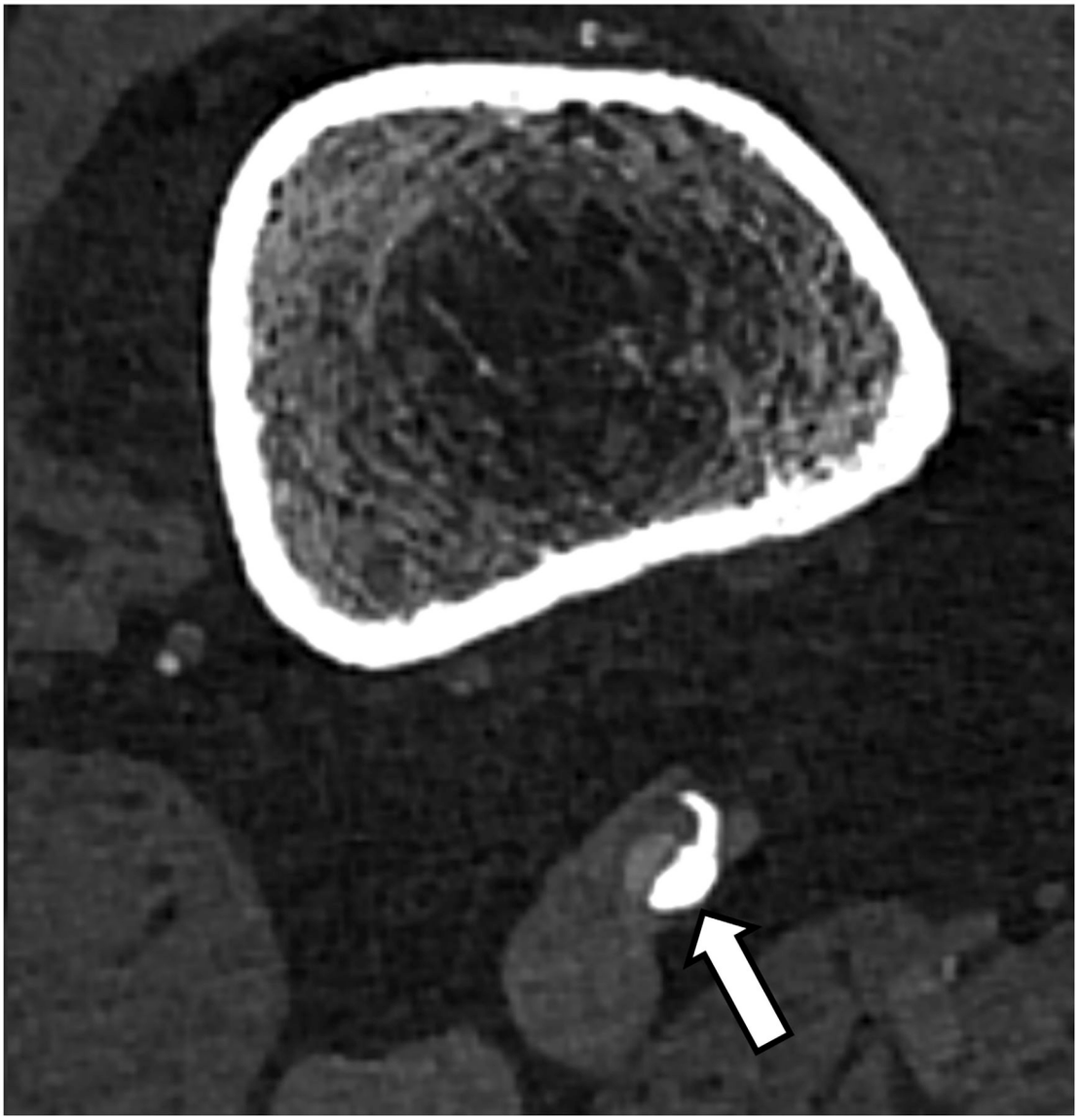

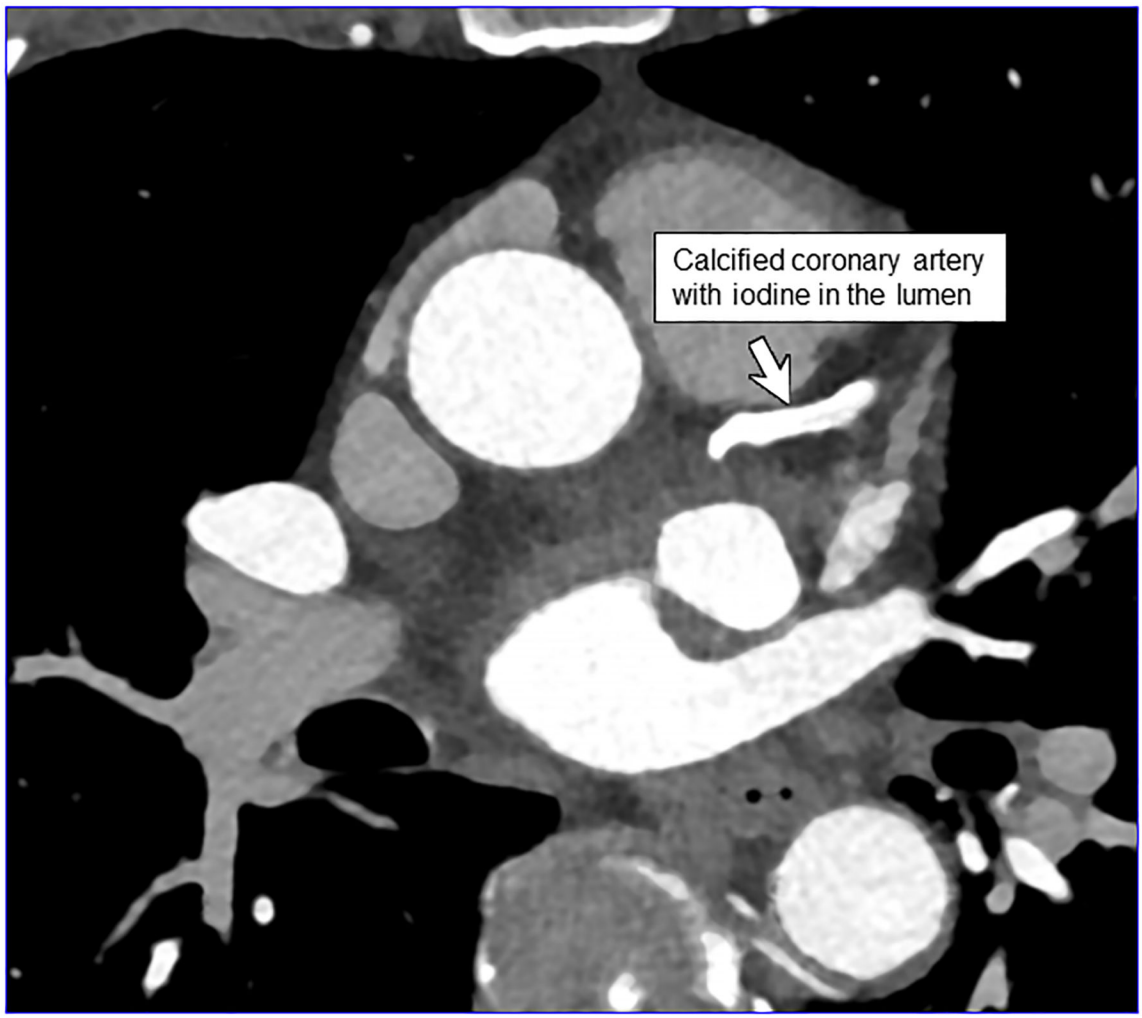

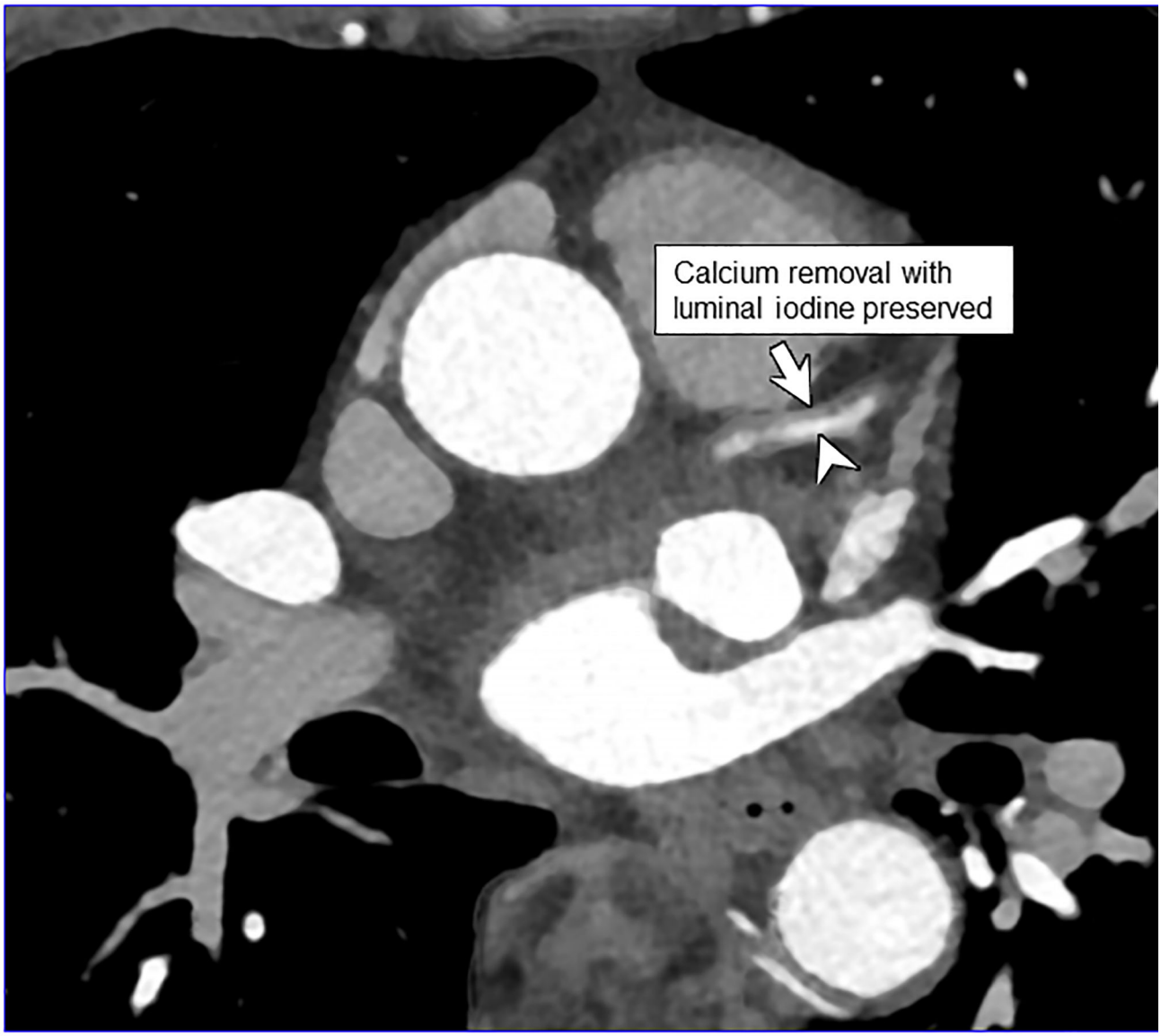

Figure 3:
EID-CT (A) and PCD-CT (120 kV PCD image comprising 20–120 keV photons, B) images from a run-off exam in a 75-year-old male demonstrate increased clarity of the lumen adjacent to the better delineated calcified plaque. PCD-CT coronary artery images in a 71-year-old male without (C) and with multi-energy post-processing (D) using an algorithm that performs material decomposition and removes calcium signal. The post-processed image (D) shows the patent lumen adjacent to the heavily calcified plaque (arrowhead). [EID: energy integrating detector; PCD: photon-counting-detector]

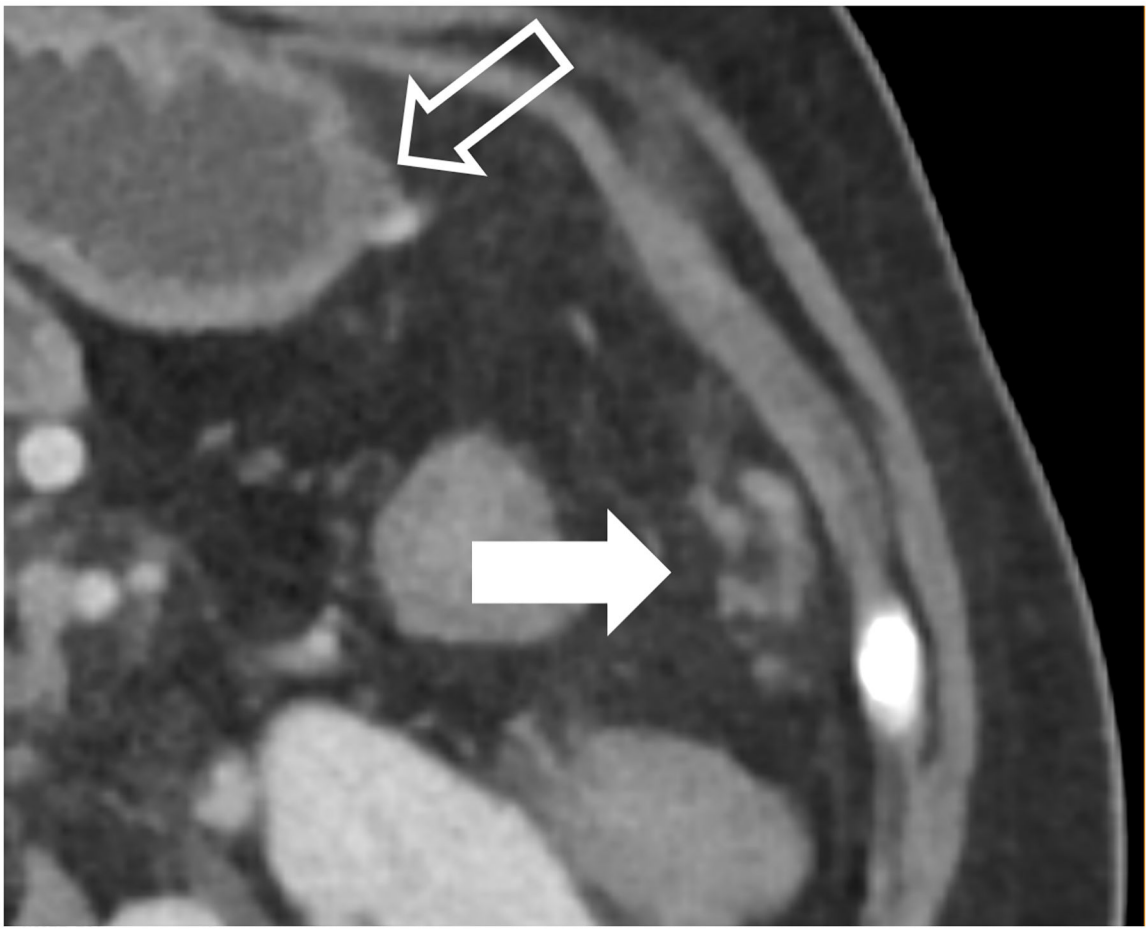

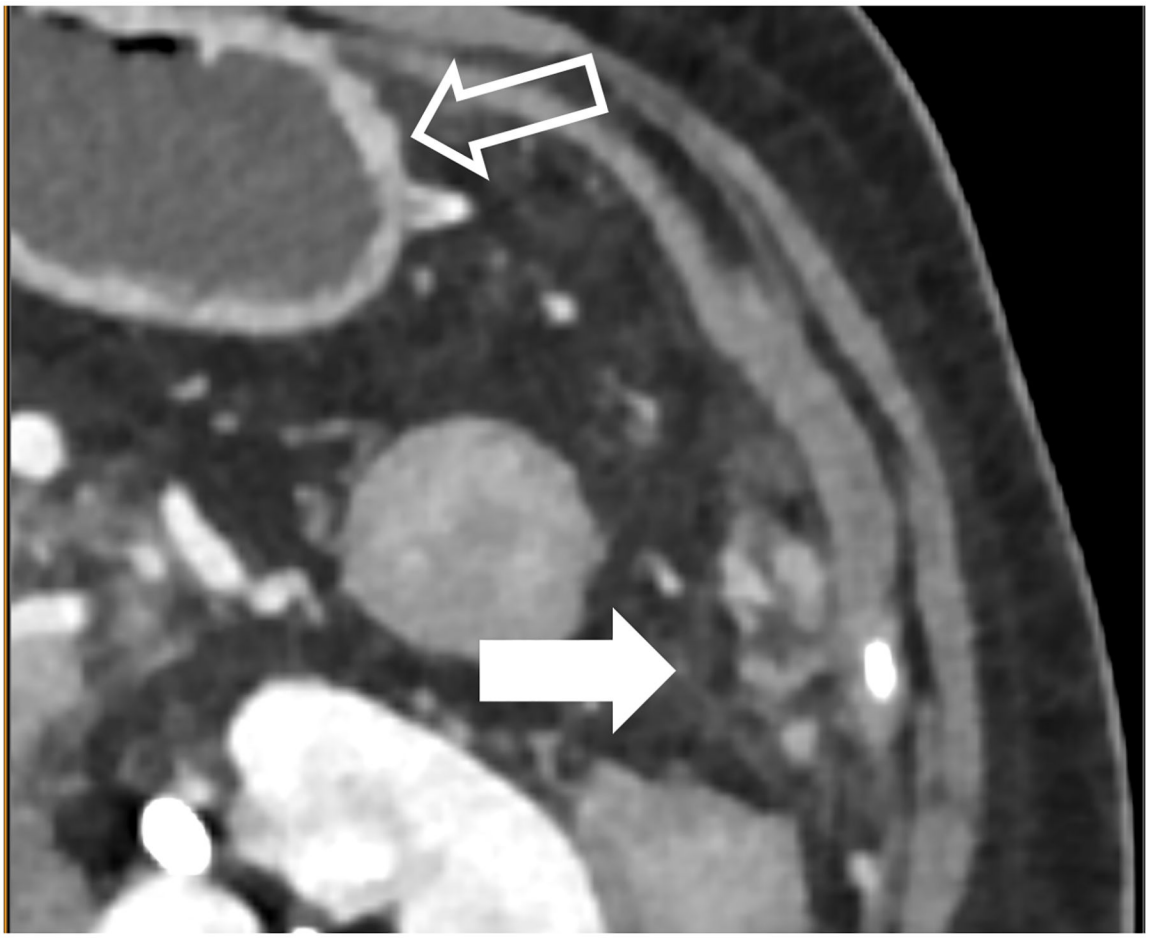

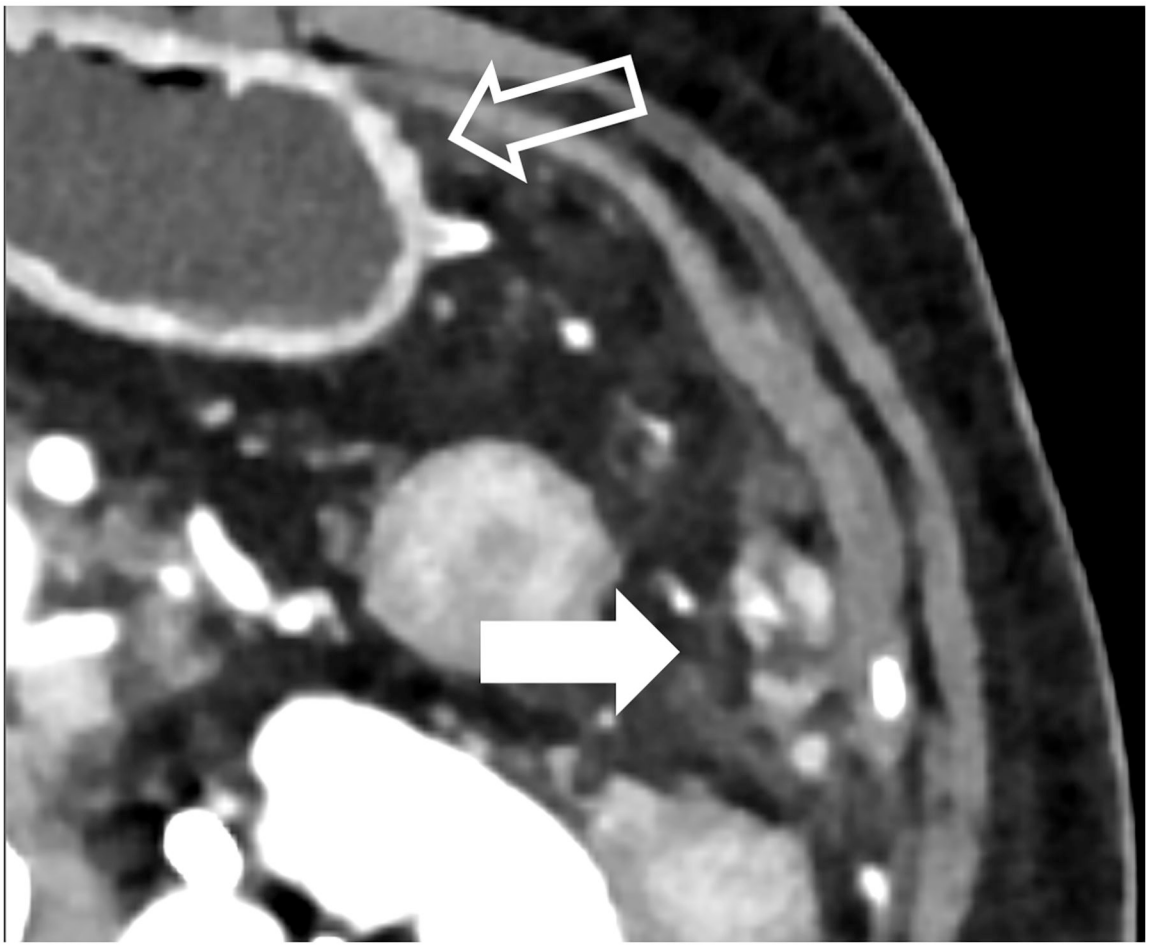

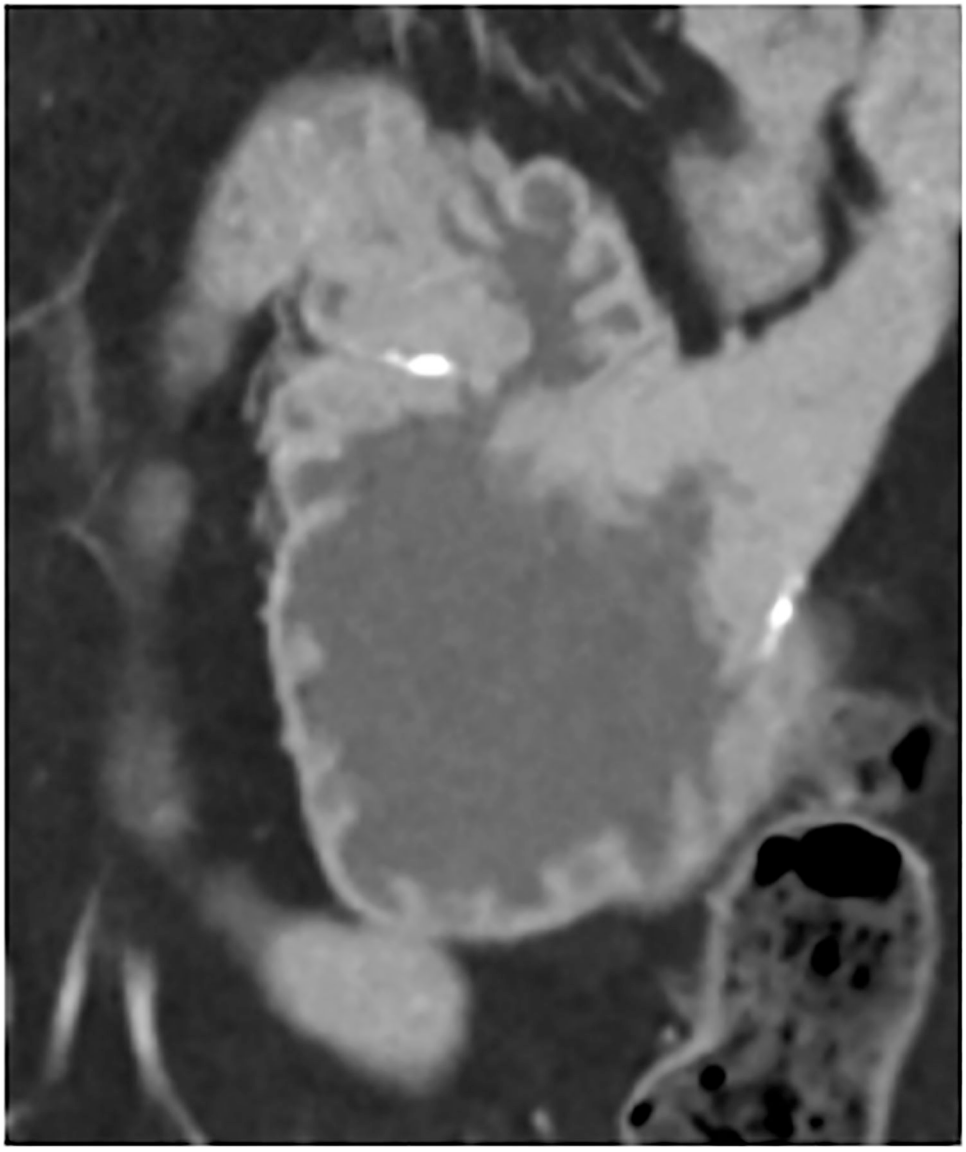

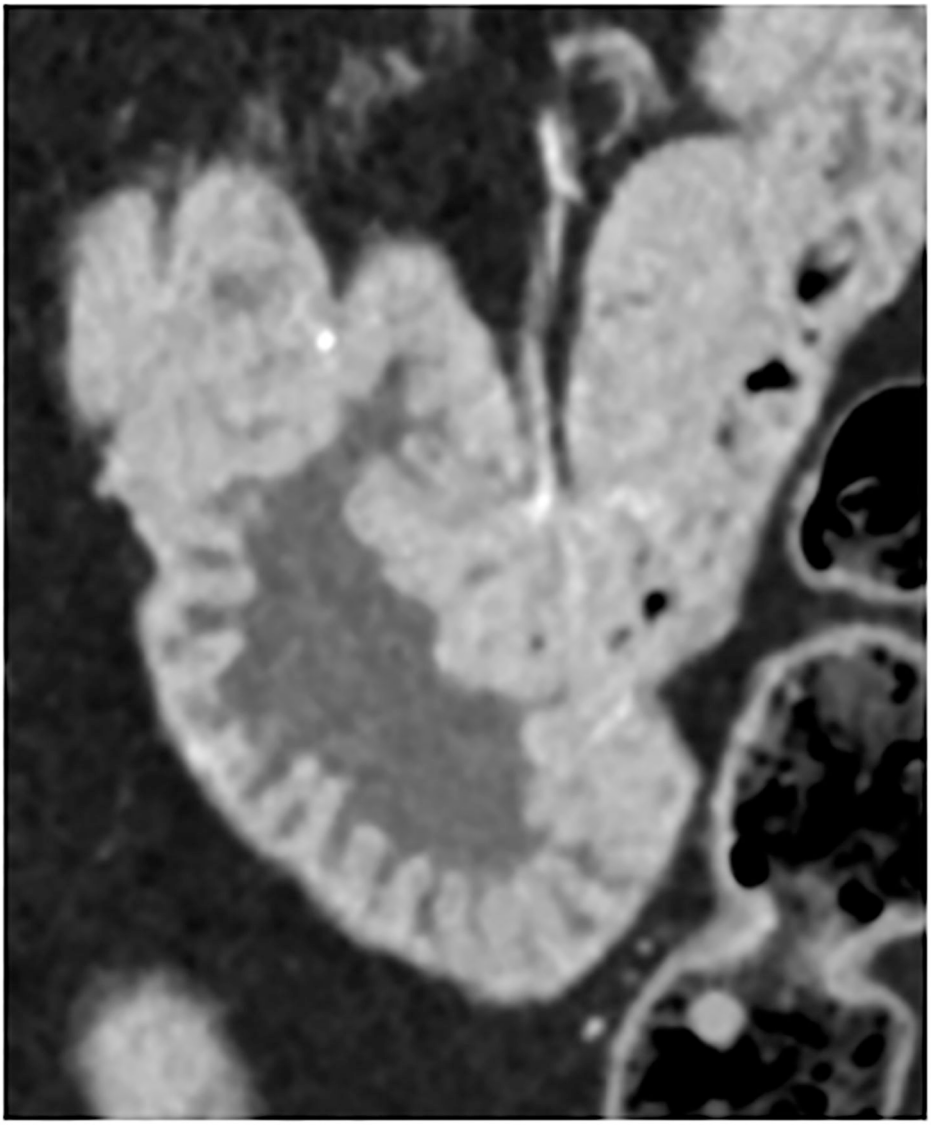

Figure 4:

Improved visualization for abdominal diagnostic tasks resulting from improved spatial resolution and/or iodine contrast. EID-CT with intravenous contrast shows a 52-year-old female with peritoneal disease from colon cancer (A, white arrow). Note visualization of the gastric wall (A, open arrow). PCD-CT shows improved iodine signal in the gastric wall and peritoneal deposits (B, open and white arrow, respectively), with iodine signal further enhanced using 50 keV virtual monoenergetic images (C). Bottom row shows impact of improved spatial resolution, with depiction of more renal stones in a 72-year-old man despite similar 2-mm slice thickness (D, EID-CT; E, PCD-CT), and improved enhancement and visualization of jejunal folds in a 70-year-old female (F, EID-CT; G, PCD-CT). PCD-CT images B, E, and G were acquired at 120 kV and comprise 20–120 keV photons. [EID: energy integrating detector; PCD: photon-counting-detector]

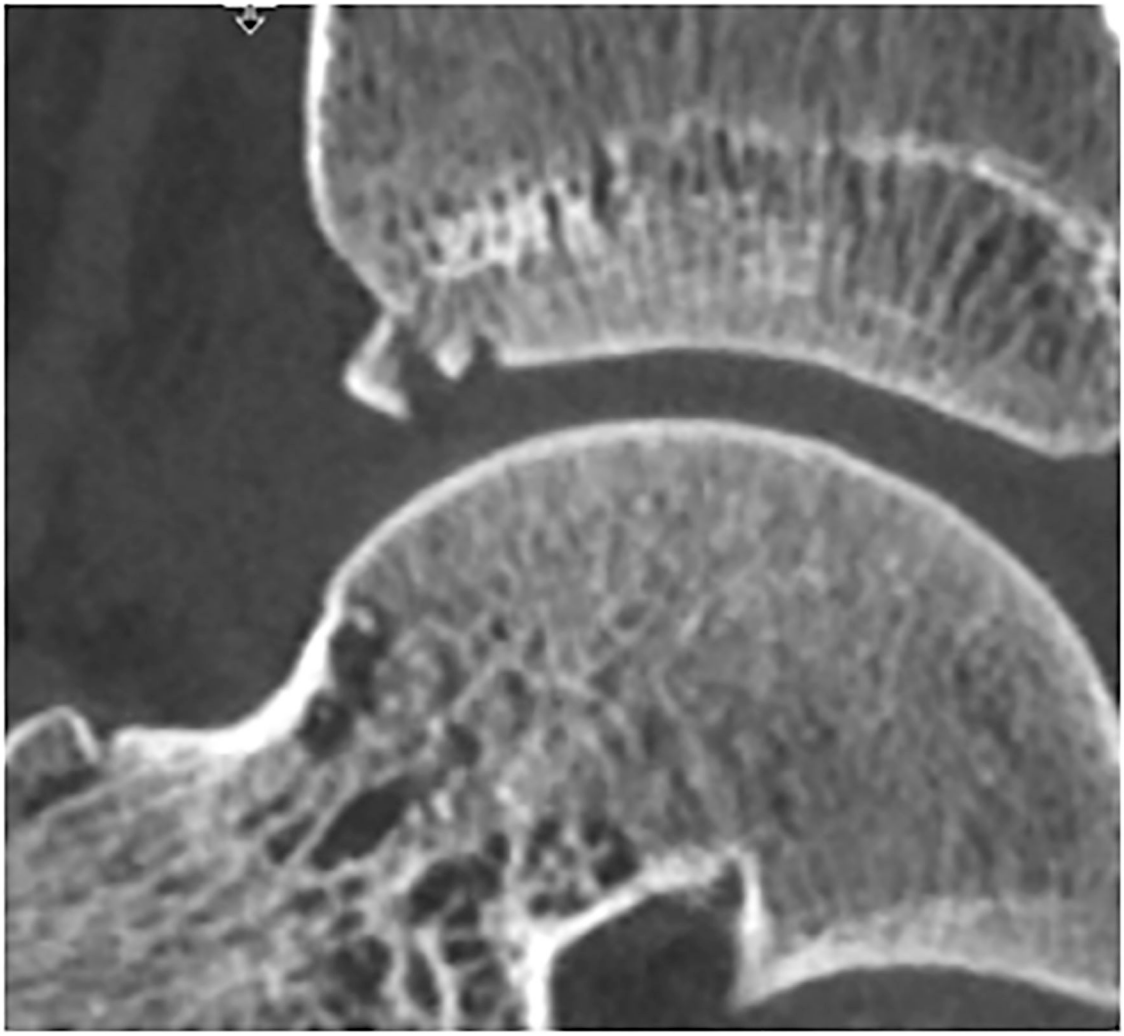

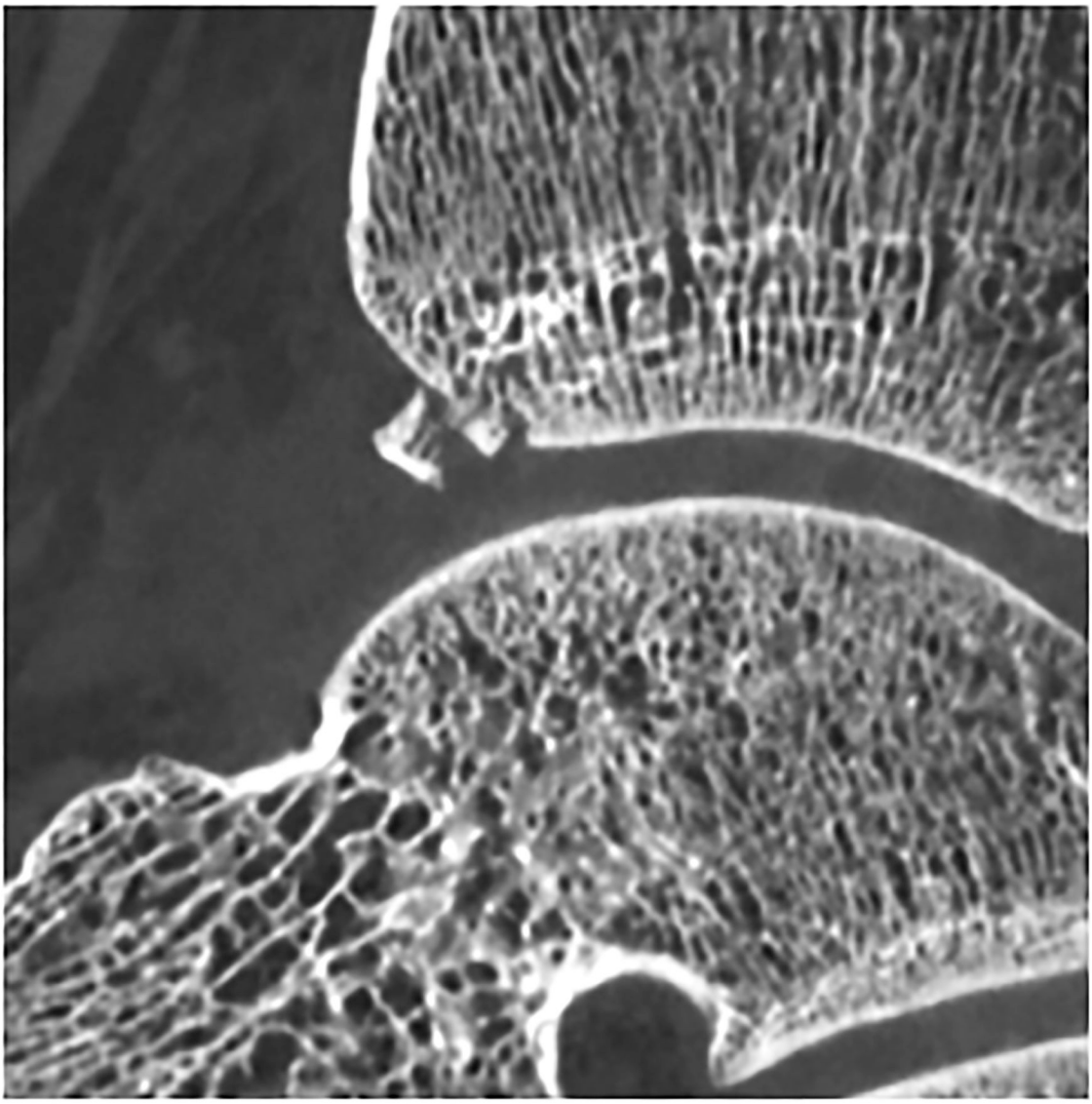

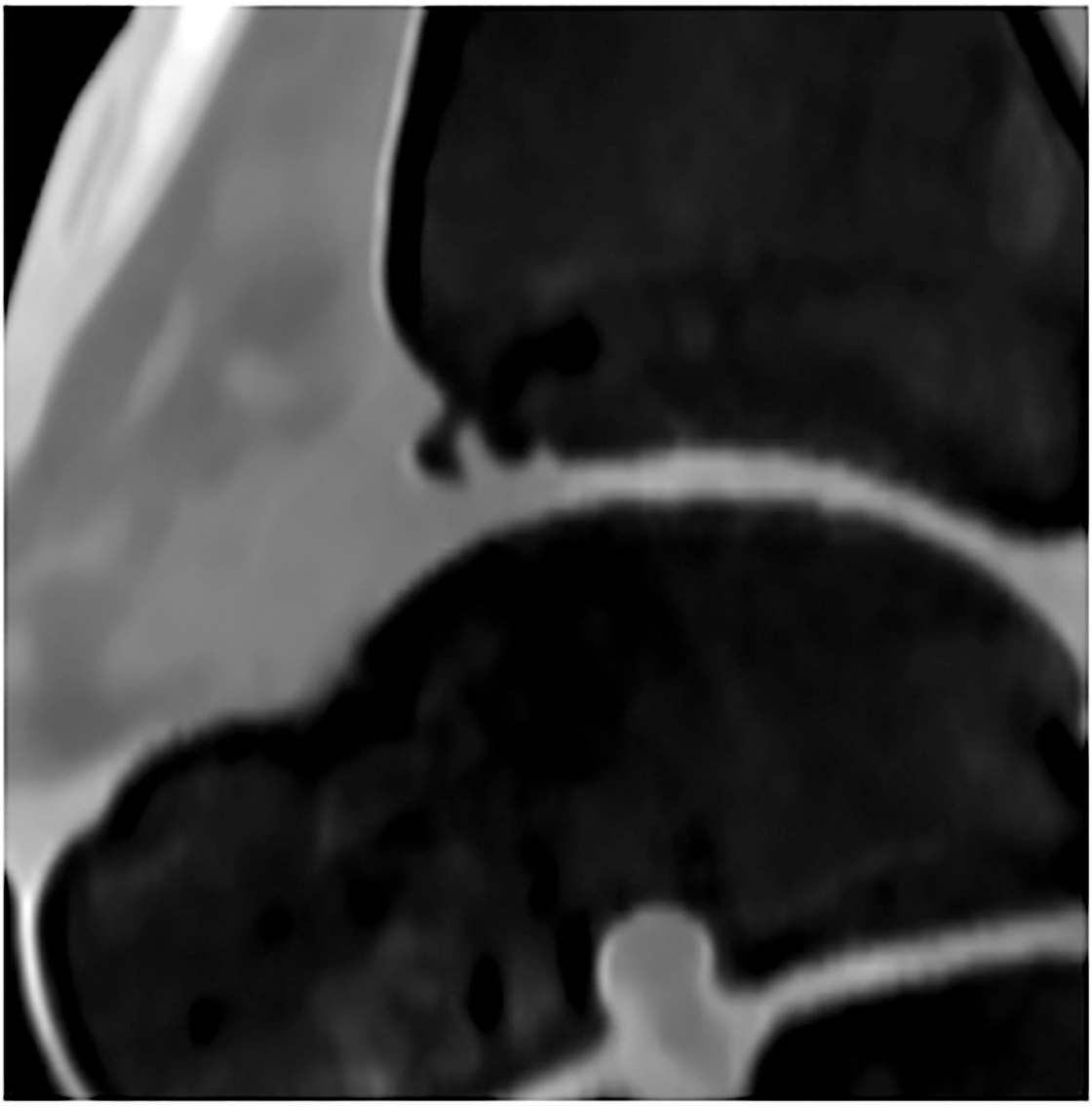

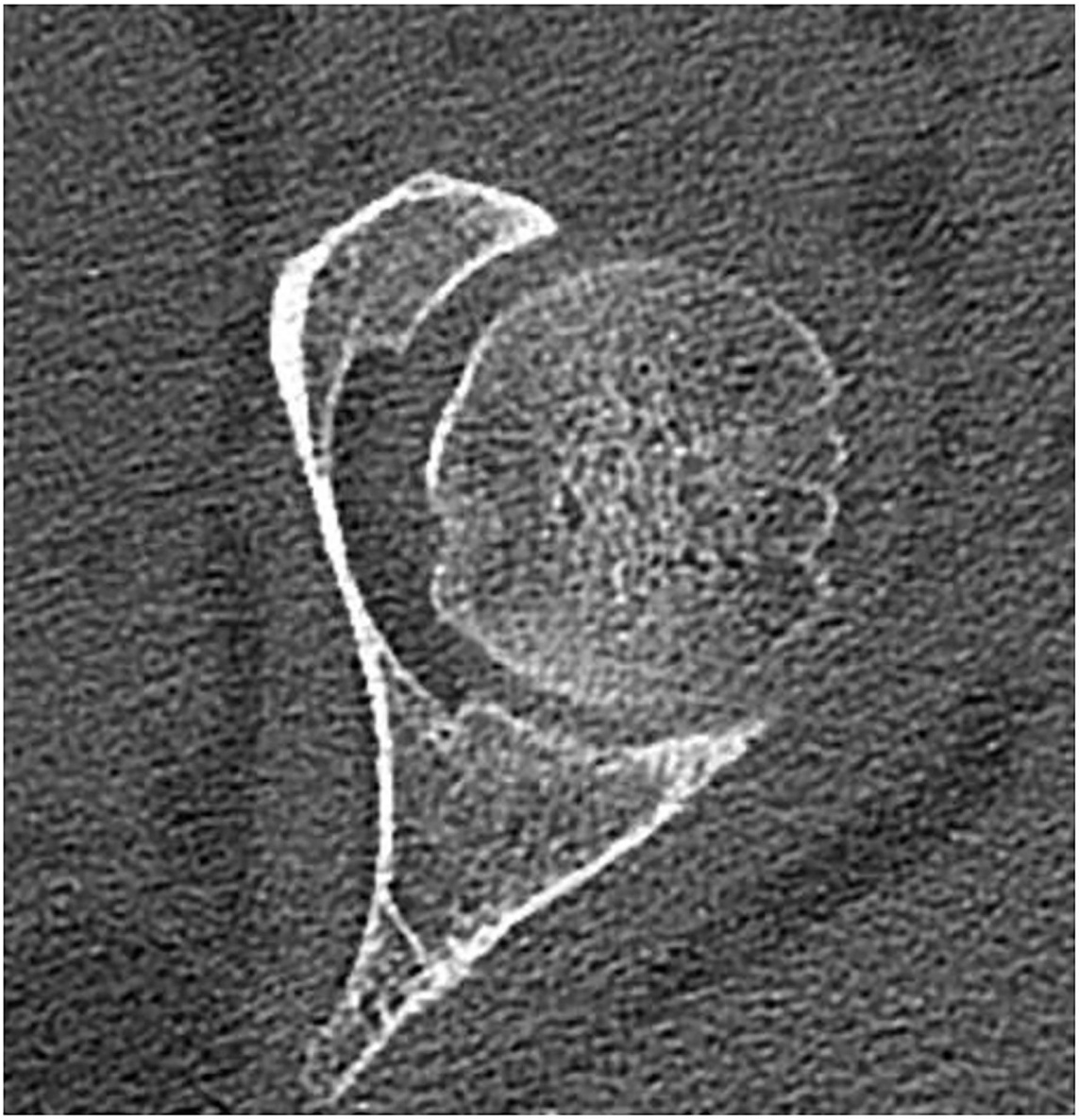

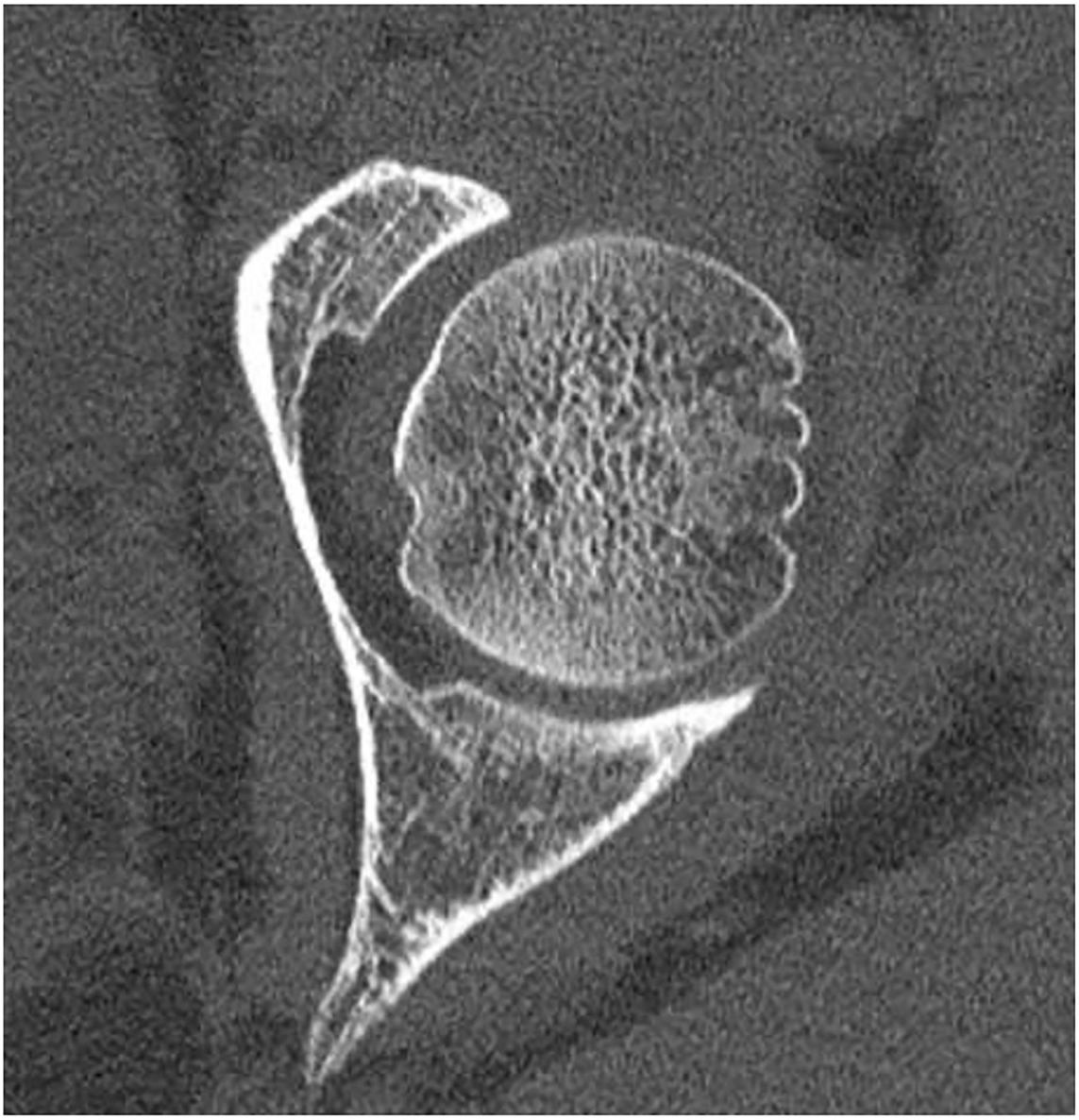

Figure 5:
Improved visualization of trabecular visualization relative to EID-CT (A) is shown on PCD-CT (140 kV PCD image comprising 20–140 keV photons, B) in images of an 18-year-old female with a cortical fracture of the anterior tibia. A multi-energy virtual non-calcium PCD-CT image (C) of the same patient was formed to look for bone marrow edema. EID-CT (D) image of the femoral head and acetabulum show decreased sharpness and trabecular structure to the PCD-CT (140 kV PCD image comprising 20–140 keV photons, E) image in a 41-year-old female. [EID: energy integrating detector; PCD: photon-counting-detector]

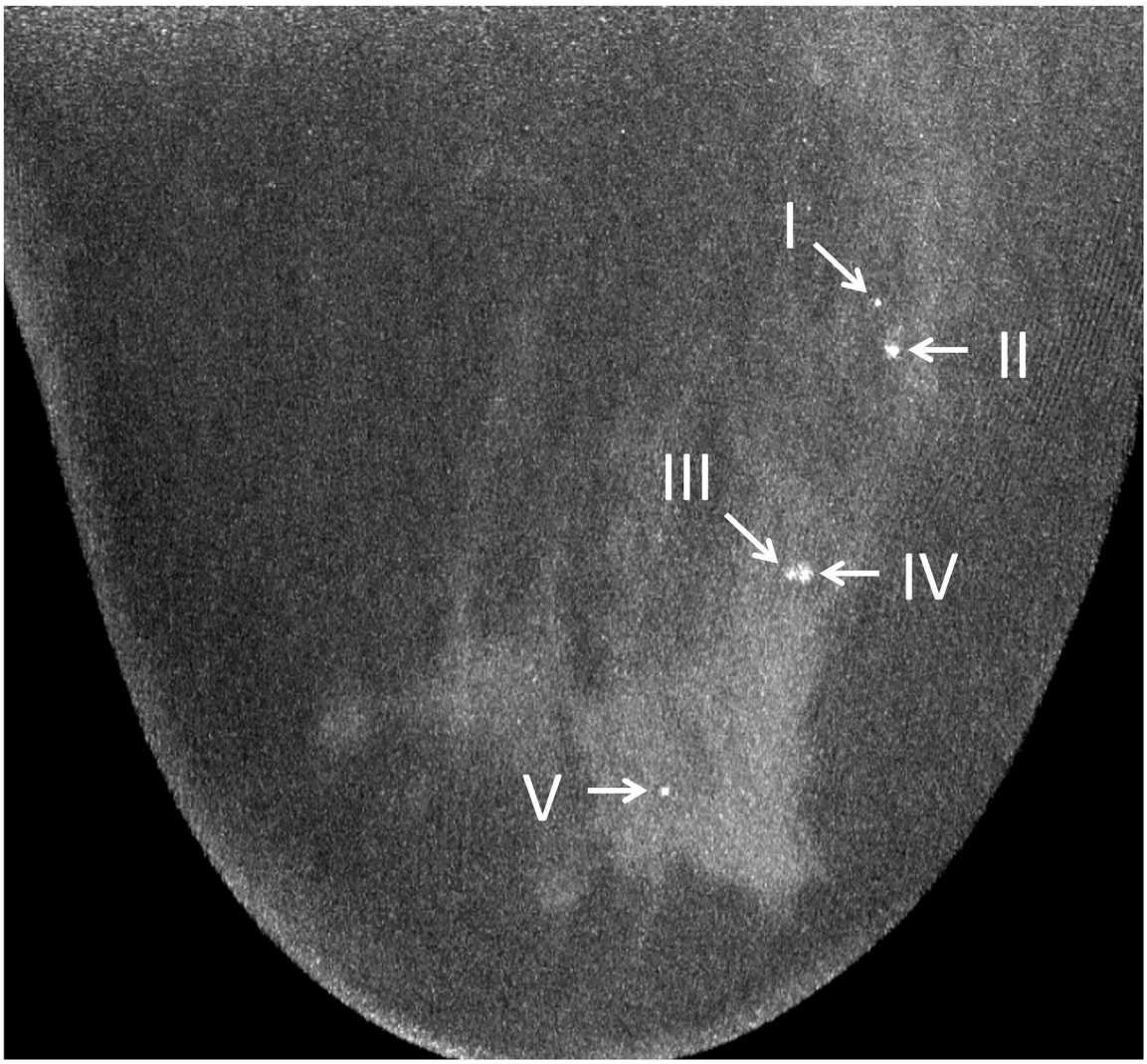

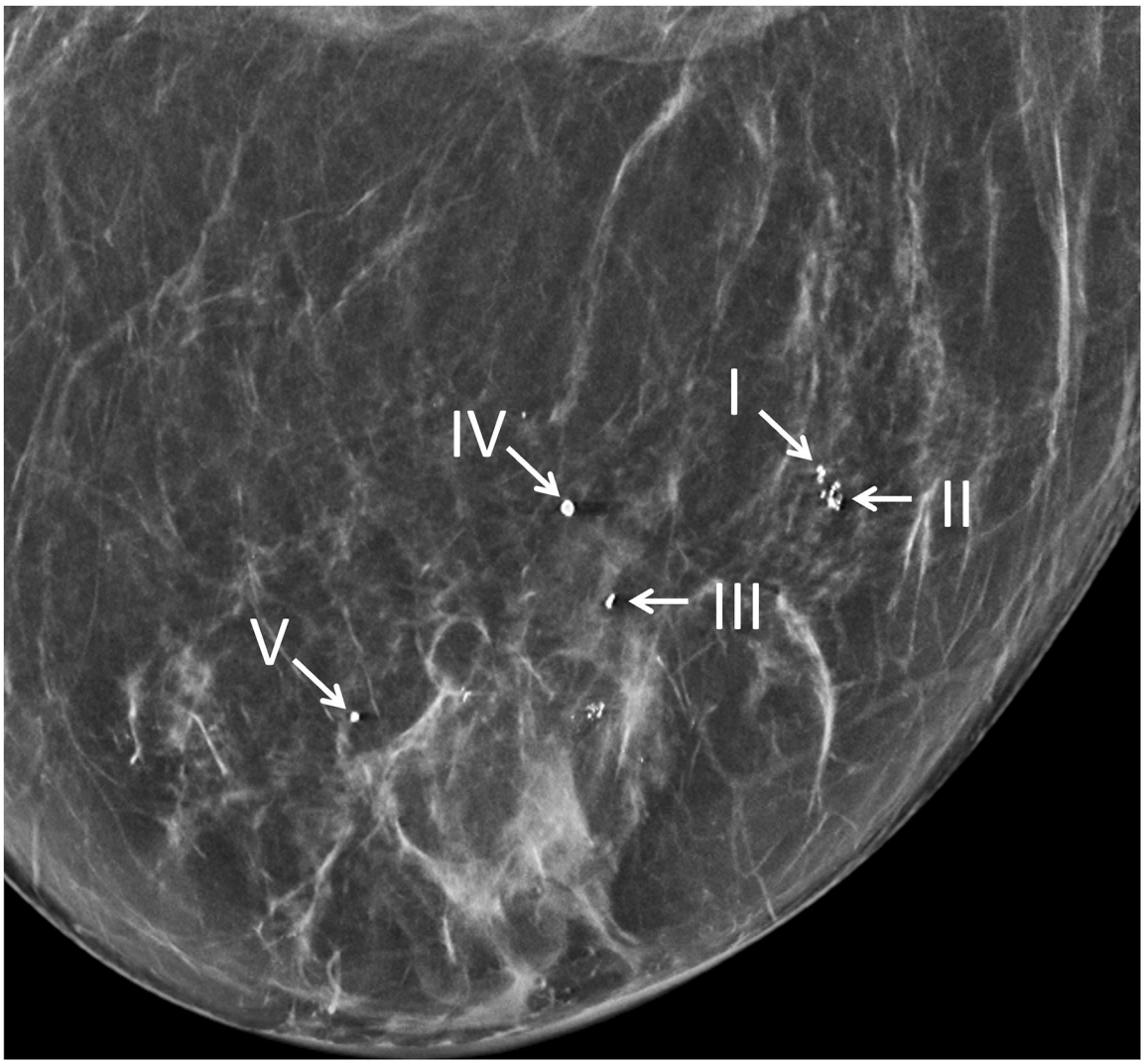

Figure 6:
Maximum intensity projection (20 mm) of ultra-high-resolution PCD-CT (120 kV PCD image comprising 20–120 keV photons) processed using CNN (A) and a clinically indicated mammographic image (B) on a 66-year-old year female. A total of five microcalcifications were detected in the PCD-CT exam following CNN noise reduction. The mammographic reference exam confirmed the presence of these microcalcifications. [PCD: photon-counting-detector, CNN: convolutional neural network]